Controlling Central Carbon Metabolism for Improved Pathway Yields in Saccharomyces cerevisiae

Citation: Tan, Sue Zanne, Shawn Manchester, and Kristala L. J. Prather. "Controlling Central Carbon Metabolism for Improved Pathway Yields in Saccharomyces Cerevisiae." ACS Synthetic Biology 5.2 (2016): 116–124.

As Published: http://dx.doi.org/10.1021/acssynbio.5b00164

Publisher: American Chemical Society (ACS)

Persistent URL: http://hdl.handle.net/1721.1/106893

Version: Author's final manuscript: final author's manuscript post peer review, without publisher's formatting or copy editing

Controlling Central Carbon Metabolism for Improved Pathway Yields in *Saccharomyces cerevisiae*

Sue Zanne Tan[1,2], Shawn Manchester[1,4] and Kristala L. J. Prather[1,2,3*]

[1]*Department of Chemical Engineering*

[2]*MIT Center for Integrative Synthetic Biology*

[3]*Synthetic Biology Engineering Research Center (SynBERC)*

Massachusetts Institute of Technology, Cambridge, MA, 02139 USA

[4]Present address: Zymergen, Inc., 6121 Hollis Street, Suite 700, Emeryville, CA 94608, USA

*Corresponding author:

Department of Chemical Engineering

77 Massachusetts Avenue

Room E17-504G

Cambridge, MA 02139

Phone: 617.253.1950

Fax: 617.258.5042

Email: kljp@mit.edu

Abstract

Engineering control of metabolic pathways is important to improving product titers and yields. Traditional methods such as overexpressing pathway enzymes and deleting competing ones are restricted by the interdependence of metabolic reactions and finite nature of cellular resources. Here, we developed a metabolite valve that controls glycolytic flux through central carbon metabolism in *Saccharomyces cerevisiae*. In a Hexokinase 2 and Glucokinase 1 deleted strain (*hxk2Δ glk1Δ)*, glucose flux was diverted away from glycolysis, and into a model pathway, gluconate, by controlling the transcription of Hexokinase 1 with the tetracycline transactivator protein (tTA). A maximum 10-fold decrease in hexokinase activity resulted in a 50-fold increase in gluconate yields, from 0.7% to 36% mol/mol glucose. The reduction in glucose flux resulted in a significant decrease in ethanol by-production that extended to semi-anaerobic conditions, as shown in the production of isobutanol. This proof-of-concept is one of the first demonstrations in *S. cerevisiae* of dynamic redirection of glucose from glycolysis and into a heterologous pathway.

Keywords: Dynamic control; Hexokinase; Transcriptional regulation; Tetracycline transactivator protein (tTA); Metabolic engineering

Introduction

Microbial fermentation has the potential to produce valuable compounds, such as pharmaceuticals[1], fragrances[2], and fuel-like molecules[3], from simple and inexpensive starting materials. One of the challenges in manufacturing molecules with microbes is achieving sufficient titers and yields such that the overall process can be economically feasible. Some common methods to improve pathway yields include overexpression of pathway enzymes[4], deletion of competing pathways[5], and engineering redox and energy balances[6]. However, these methods are not always successful due to the interconnectivity of metabolic pathways and the finite nature of cellular resources[7]. Deletion of competing pathways may deprive cells of essential metabolites that would have to be supplied extracellularly to support growth, which creates an undesirable added expense for the culture medium. On the other hand, simply overexpressing pathway enzymes comes at the expense of shared cellular resources, such as ATP and NAD(P)H that ultimately lead to poor growth and protein expression[8], especially if these enzymes are kinetically inferior to endogenous ones.

An alternative to these traditional approaches is to control and regulate metabolic pathways in a dynamic manner[9]. Here, synthetic biology offers tools such as inducible gene expression systems[10] and quorum sensing circuits[11] that enable the construction of pathway regulation. Although these genetic circuits are well studied, there remains a gap in effectively integrating these systems into different levels of cellular complexity. Recent efforts in utilizing synthetic biology tools in metabolic control have mainly focused on *Escherichia coli* as a host. Dynamic regulation of carbon flux at glycolysis using a genetic inverter[12] and by controlled enzyme degradation[13] have been shown by our lab, while others have explored nodes further down in central carbon metabolism such as the construction of a malonyl-CoA sensor[14],

optimization of enzyme expression levels for fatty acid production[15], and a toggle switch at the acetyl-CoA node of the TCA cycle[16]. In *Saccharomyces cerevisiae* however, successful implementation of synthetic regulatory circuits for metabolic control remains challenging. Most studies have involved relatively simple circuits using native promoter systems that are dependent on cellular metabolites such as methionine[17–19] or galactose[20]. Such systems that involve induction by native metabolites are limited in robustness. Metabolism of methionine during growth has been shown to relieve repression of the gene under MET3 promoter control, leading to a decrease in product synthesis[21]. Circuits involving the GAL promoter are limited to systems where changing carbon sources between glucose and galactose is permissible, thereby excluding most production strains where carbon sources can significantly affect metabolic enzyme activities[22] and heterologous gene expression[23]. More recently, dynamic regulation using native pheromone quorum sensing has been shown to improve production of para-hydroxybenzoic acid (PHBA)[24]; however, the system was restricted to tryptophan-free media since addition of tryptophan was used to initiate the quorum sensing system. In addition, most metabolic control efforts in *S. cerevisiae* have concentrated on increasing flux through the farnesyl diphosphate branch-point, where the MET3[18] and ERG1[25] promoters were used to improve amorphadiene titers and the HXT1 promoter to increase α-santalene production[19]. Outside of the mevalonate pathway, little has been accomplished in controlling central carbon metabolism for pathway improvements. Although early glycolysis and its role in glucose repression[26] and ethanol accumulation[27] are well studied, redirecting carbon flux at this node into a heterologous pathway, when no other carbon source exists, remains unexplored.

The first committed step of glycolysis involves the conversion of glucose to glucose-6-phosphate with the consumption of ATP. In *S. cerevisiae*, this step is catalyzed by three

enzymes: hexokinase 2 (Hxk2p), hexokinase 1 (Hxk1p) and glucokinase 1 (Glk1p)[28]. Hxk2p is the dominant enzyme that is involved in glucose repression and represses the expression of Hxk1p and Glk1p in the presence of glucose[29]. We hypothesized that controlling the enzyme levels responsible for this first step of glycolysis would enable the control of carbon flux into central carbon metabolism when glucose is the sole carbon source. In particular, knocking down hexokinase or glucokinase levels will reduce the amount of glucose-6-phosphate available for glycolysis, thereby increasing the availability of glucose. Here, we present a genetically encoded metabolite valve[12] that provides the control of central carbon metabolism and redirection of carbon flux into a heterologous pathway. We first constructed a *hxk2*Δ *glk1*Δ strain and controlled the only remaining Hxk1p using the tetracycline transactivator protein (tTA) system[30]. Unlike native promoter systems, this synthetic gene repression system is repressed by the addition of doxycycline, which is not metabolized by cells, thereby providing a more stable regulatory system. To then demonstrate the redirection of flux into a heterologous pathway, we chose production of gluconic acid, or gluconate, as a model pathway that utilizes glucose as the substrate. Gluconic acid is widely used as a bulk chemical in food, feed, and textile industries[31]. It is commercially made through a variety of different manufacturing processes: chemical synthesis, electrochemical catalysis, and enzymatic biocatalysis, as well as fermentation processes using bacteria or fungi[32]. Some examples of microbial fermentation of gluconic acid are from *Aspergillus niger*[31] and *Aureobasidium pullulan* [33], where yields of up to 95% and 87% on glucose were achieved at optimized conditions. Glucose can be converted to gluconic acid through an oxidation process to glucono-δ-lactone, which spontaneously hydrolyzes to gluconic acid. We expressed glucose dehydrogenase, *gdh*, from *Bacillus subtilis* for the production of gluconic acid in our strains. The reported k_{cat}/K_M value of *B. subtilis* glucose dehydrogenase, 160

M/s[34], is significantly lower than that of *S. cerevisiae* Hxk1p, 8800 M/s[35,36]. Since Hxk1p intrinsically outcompetes glucose dehydrogenase for glucose, this pathway is an ideal model system to demonstrate the utility of a glucose valve. This proof-of-concept is one of the first demonstrations in *S. cerevisiae* of dynamically redirecting glucose flux away from glycolysis, resulting in superior improvement in yields (50-fold) of a heterologous pathway while simultaneously reducing ethanol by-production even in glucose excess conditions. Moreover, we extended the application of this system to improving yields of the isobutanol pathway. Even in semi-anaerobic conditions, a 30% decrease in ethanol accumulation was achieved, alongside a 3-fold increase in isobutanol yield from glucose.

Results and Discussion

Repression of Hexokinase Activity Increases Gluconate Yields

In a *hxk2*Δ *glk1*Δ strain, Y12 (Table 1), we constructed a glucose valve at the only remaining hexokinase, Hxk1p, to divert flux away from central carbon metabolism and into the gluconate pathway (Figure 1A). We hypothesized that deleting the dominant and regulatory Hxk2p would disrupt native regulation of glucose, thereby allowing the valve more control over carbon flux at this node. The transcription of HXK1 and GLK1 has been shown to be up-regulated in *hxk2Δ* mutants with glucose as the carbon source[37]; therefore, we predicted that the deletion of this dominant Hxk2p would still result in sufficient flux into glycolysis to support growth and production. The valve was constructed by controlling the transcription of HXK1 using the tetracycline transactivator protein (tTA) system (Figure 1B). The tTA system has been shown to repress transcription, upon addition of doxycycline (dox), up to 100-fold using β-galactosidase as a reporter[38]. We first tested this system in a positive feedback manner, with tTA being expressed under 7xtetO in the genome, driving the expression of YFP with 7xtetO on a centromeric plasmid. Addition of dox repressed YFP fluorescence in a dose-dependent manner and up to a maximum 80% (Figure S1, Supporting Information). In addition, we estimated the burden of expressing the tTA system by comparing the growth of Y15 (*hxk2Δ glk1Δ* trp1::7xtetO tTA) to Y12 (*hxk2*Δ *glk1*Δ) and saw small effects on growth but comparable final OD_{600} (Figure S2, Supporting Information).

To control the transcription of HXK1 with the tTA system, we expressed 7xtetO tTA in the genome and replaced the native HXK1 promoter in Y12 with 7xtetO, creating strain Y17. Addition of dox repressed hexokinase activity up to 10-fold, as measured in cell lysates at late exponential phase (Figure 2A). The repressed hexokinase activity of strains with 500-2500

ng/mL dox persisted into stationary phase, while those with 0-250 ng/mL dox increased when measured at stationary phase. The general increase in hexokinase activity from exponential to stationary phase is consistent with previous reports[39]; hexokinase activity of wild-type *S. cerevisiae* has been shown to increase 5-fold throughout growth. This result suggested that a minimum amount of 500-1000 ng/mL dox was needed to maintain hexokinase repression up to 72 hours and concentrations above 1000 ng/mL provided no additional repression; therefore, subsequent experiments were performed with 1000 ng/mL dox. mRNA quantification of HXK1 confirmed that the reduction in hexokinase activity was due to reduced HXK1 mRNA levels (Figure 2B). HXK1 mRNA levels were significantly lower in strains with dox addition, up to ~100-fold at 1000-2500 ng/mL dox, at both late exponential and stationary phases.

Although mRNA levels alone have been shown to be insufficient in predicting protein abundance in *S. cerevisiae*[40,41], the decrease in HXK1 mRNA levels was consistent with the observed trend in hexokinase activity in our experiments. In addition, it has been reported that transcription only accounts for 30% of the regulation of Hxk1p abundance[42]; by measuring glycolytic fluxes, it was determined that Hxk1p and other glycolytic enzymes were primarily regulated at post-transcriptional levels. Here, we saw that a 100-fold decrease in mRNA levels resulted in a 10-fold decrease in hexokinase activity at late exponential phase (although at stationary phase, a 100-fold decrease was observed primarily due to an increase in activity of the non-induced strain). The relationship between HXK1 mRNA levels and the observed activity of Hxk1p is also complicated by its direct effect on growth rate. Down-regulation of Hxk1p decreases growth rate that counters the effects of dilution by growth. In fact, simple modeling using experimental growth rates and literature values of Hxk1p translation rate[43], mRNA synthesis rate and half-life[44] supports this hypothesis (Figure S3, Supporting Information). The

model shows that an 80% reduction in mRNA synthesis rate only results in a 46% reduction in activity due to growth-mediated buffering effects of Hxk1p, while incorrectly assuming a constant growth rate predicts a higher, 79%, reduction in activity instead. This similar effect has been demonstrated in the down-regulation of glucokinase in a *ΔptsHIcrr E. coli* strain[12].

After demonstrating effective hexokinase repression, the gluconate pathway was introduced into WT W303 and Y17 strains by expressing glucose dehydrogenase on a centromeric plasmid, pRS415-*gdh*. Gluconate titers and yields were lower in Y17 than in WT, though not substantially so (Figure 2C-D). Although Hxk2p and Glk1p were deleted in Y17, the measured hexokinase activity of Y17 was higher than that in Y12 (Figure S4, Supporting Information). This result suggests that 7xtetO tTA, with a CYC1 TATA box, is a stronger promoter than the native HXK1 promoter in Y12, resulting in hexokinase expression levels that were more comparable to WT levels. However, upon induction of Y17 with 1000 ng/mL dox at OD_{600} 0.01, there was a significant increase in gluconate titers from 0.15 g/L to 1.8 g/L (Figure 2C). More importantly, a ~50-fold increase in gluconate yields from glucose was achieved, from 0.7% to 36% mol gluconate/mol glucose. This large improvement in yield is the result of both an increase in gluconate titers and a significant decrease in glucose consumption in the induced strains. In comparison to reported industrial yields of 87-95%[31,33], this improved yield of 36% was achieved in shake flask experiments without any other strain or process optimization. The repression of hexokinase activity successfully allowed glucose flux to be redirected into the gluconate pathway, even when the reported k_{cat}/K_M of the competing native Hxk1p was more than an order of magnitude higher than the heterologous glucose dehydrogenase[34–36]. In addition, the 10-fold decrease in hexokinase activity through transcriptional control was sufficient for the redirection of glucose, even though it was reported that transcription only accounts for 30% of

the regulation of Hxk1p abundance[42]. Thus, we believe that our tTA system is generalizable to enzymes that are regulated at the transcriptional level, even if transcription may only account partially for its regulation of abundance. To confirm that the observed increase in gluconate titers is not due to an increase in the activity of the pathway enzyme but due to repression of hexokinase activity, glucose dehydrogenase activities were measured in Y17 at different dox concentrations (Figure S5, Supporting Information). There was no increase in glucose dehydrogenase activities at high dox concentrations where significant improvement of gluconate titers and repression of hexokinase activity were observed. This experiment confirmed that the increase in gluconate titers was not simply due to higher activity of the pathway enzyme, but due to glucose redirection as designed.

Control of Glucose Flux to Production versus Growth

We further characterized gluconate production of Y17 under different inducer concentrations and timing of induction (Table S1, Supporting Information). Under these various conditions, a range of different growth rates and gluconate titers was achieved, ranging from 0.05-0.10 hr^{-1} and 0.08-2.31 g/L gluconate, respectively (Figure S6, Supporting Information). In general, higher dox concentrations and earlier induction times resulted in strains with the lowest hexokinase activities. At low levels of hexokinase activities, these strains grew more slowly, presumably due to reduced flux into glycolysis. A triple null mutant of *hxk1*Δ, *hxk2*Δ, and *glk1*Δ failed to grow on glucose as the sole carbon source, confirming that no other carbon utilization routes exist at these experimental conditions. Therefore, the observed changes in growth rates solely due to change in hexokinase activities in our experiments are reflective of glycolytic flux.

Strains with the slowest growth rates were the highest gluconate producers; less glucose flux into glycolysis allowed more glucose to be redirected into the gluconate pathway.

In addition to producing a range of different gluconate titers, these strains also produced different amounts of ethanol at late exponential phase (Figure S7, Supporting Information). Strains with the lowest growth rates generally produced the least amount of ethanol, consistent with studies on the Crabtree effect at glucose-limited conditions[45]. The formation of ethanol in *S. cerevisiae* even in aerobic conditions is due to overflow metabolism; at high glycolytic flux, fermentation occurs due to limitations in respiratory capacity[27]. Glycolytic flux, in turn, depends on the glucose uptake rate which is regulated by a family of hexose transporters. These hexose transporters are encoded by the twenty HXT genes, each with different glucose affinities and is regulated by extracellular glucose concentrations[46,47]. Due to these reasons, culturing *S. cerevisiae* at glucose-limited conditions has been used to prevent ethanol by-production[48]. Here, we show that ethanol production can be prevented even at high glucose concentrations of 20 g/L, by solely controlling the expression of Hxk1p. Previous efforts at controlling glucose flux to prevent ethanol production involved the construction of a chimeric transporter of Hxt1p and Hxt7p in a background where all other hexose transporters had been deleted[49]. Instead of controlling glucose uptake rate, we show that controlling glycolysis directly at hexokinase is sufficient to control glucose flux such that ethanol production is significantly reduced, regardless of external glucose concentrations.

Repression of Hexokinase Activity Improves Isobutanol Yields

S. cerevisiae natively produces isobutanol, alongside other fusel alcohols, through amino acid catabolism pathways[50]. Interest in isobutanol as a next generation biofuel substitute has

motivated the engineering of *S. cerevisiae* for improved isobutanol production. Overexpression of native enzymes in the valine synthesis pathway[51–53], mitochondrial redirection of keto-acid decarboxylase (KDC) and alcohol dehydrogenase (ADH)[54], and cytosolic re-localization of valine synthesis enzymes[55] have been shown to increase isobutanol titers up to 600 mg/L and yields up to 15 mg/g glucose[55]. Nonetheless, these reported isobutanol yields are far from the theoretical yield of 0.4 g/g glucose. The significant production of ethanol as a byproduct, at yields of 0.4 g/g glucose (theoretical yield = 0.5 g ethanol/g glucose), where reported[51,56], also remains a challenge. Since both ethanol and isobutanol rely on pyruvate as a precursor (Figure S8, Supporting Information), reduced production of ethanol may increase the available pyruvate for isobutanol production. In addition, reduced ethanol accumulation also relieves its toxicity[57]. The first committed step in the conversion of pyruvate to ethanol is through acetaldehyde, catalyzed by pyruvate decarboxylase. A pyruvate decarboxylase negative strain has been constructed[58]; however, it grows poorly on glucose as a sole carbon source presumably due to the requirement of pyruvate decarboxylase for cytosolic acetyl-CoA production[59]. Aside from deleting the major pyruvate decarboxylase, Pdc1p, which did not reduce ethanol production of strains overproducing isobutanol[56], there has been little effort in preventing ethanol formation for the improvement of isobutanol yields. We have shown that repressing hexokinase activity in Y17 not only improved gluconate yields, but also diminished ethanol production at late-exponential phase. Given this ability, we investigated the applicability of the hexokinase system to improve yields of isobutanol from glucose.

First, the hexokinase system in Y17 was reconstructed in CEN.PK2, a more industrially relevant strain, generating strain Y115. In order to increase isobutanol titers, two previously reported overexpression constructs were tested in semi-anaerobic conditions: pJA123 containing

ILV2, ILV3 and ILV5, and pJA180 containing ILV2, ILV3, ILV5 and mitochondrial targeted Ll-KivD and Ll-adhA(RE1)[54]. Despite now being in semi-anaerobic conditions, Y115 still produced significantly less ethanol compared to WT (Figure 3A), consistent with results obtained with Y17 under aerobic conditions. At day 4, ethanol levels in Y115 were only 4-6 g/L compared to 46-48 g/L in WT. At day 10, ethanol levels in Y115 increased to 19-33 g/L, but still less than that of WT which remained approximately constant. Ethanol yields of WT and Y115 were 0.45 and 0.40 g/g glucose at day 10 (Figure S9, Supporting Information). As shown in Figure 3B, isobutanol titers at day 4 of WT expressing pJA123 and pJA180 were 48.9 mg/L and 34.9 mg/L, and these titers remain approximately constant through day 10. In contrast, isobutanol titers of Y115 continue to increase after day 4, resulting in 124.1 mg/L and 167.2 mg/L in pJA123 and pJA180, respectively. Taken together, the production of isobutanol in Y115 was slower, but reached significantly higher final isobutanol titers compared to WT after 10 days, while producing less ethanol. Moreover, isobutanol yields of all Y115 constructs were higher than that of WT, at both days 4 and 10 (Figure 3C), with the highest yield being 3.4 mg/g glucose for pJA180. Isobutanol yields were higher for Y115 even when titers were lower at day 4, due to reduced glucose consumption (Figure S10, Supporting Information). Measurements of other byproducts also showed increased glycerol, acetate and succinate yields in Y115 compared to WT (Table S2, Supporting Information).

Reducing glucose flux into glycolysis in Y115 resulted in decreased growth rate compared to WT. The effects of growth rate on ethanol production in glucose-limited conditions are well established[45]; below a certain growth rate, glucose metabolism is fully respiratory with no ethanol accumulation. In glucose excess conditions however, the effects of growth rate on ethanol, and isobutanol production, are unclear. To determine if reduced growth rate of WT

alone can lead to the decreased ethanol and increased isobutanol production as seen in Y115, continuous stirred tank reactor experiments were performed with WT pJA123 at dilution rates of 0.03-0.12 hr^{-1} at semi-anaerobic and glucose excess conditions. Interestingly, decreasing dilution rates of WT pJA123 increased both ethanol and isobutanol titers (Figure S11, Supporting Information), suggesting that the observed results in Y115 may not be due to reduced growth rate alone. It is worth noting that the steady state conditions in continuous reactors on WT are not fully representative of the Y115 results that were obtained in batch cultures. Besides differences in growth rate, glucose consumption of Y115 also differed significantly from WT (Figure S10, Supporting Information), since repression of hexokinase activity reduced glucose flux into glycolysis. Therefore, we sought to investigate if the high external glucose concentrations in Y115 could lead to activation of glucose repression pathways that promote amino acid biosynthesis[28], which may drive more flux into the isobutanol pathway. The Gcn4p transcriptional activator is known to activate amino acid metabolism[60], including induced expression of ILV2[61]. Because regulation of Gcn4p is mainly at the translational level, we sought to quantify Gcn4p levels in WT and Y115. However, we failed to obtain bands on the Western Blot, most probably due to its low levels and short half-life of ~5 min under non-induced conditions[62]. Measurements of Ilv2p's acetolactate synthase activity (Figure S12, Supporting Information) showed no differences between Y115 compared to WT, suggesting that upregulation of Ilv2p in Y115 was unlikely. These results indicate that the observed increase in isobutanol titers in Y115 is likely not due to increased expression of Ilv2p alone.

Lastly, to investigate if the deletion of Hxk2p in Y115 played a role in the increased isobutanol titers, *hxk2Δ* only strains (Y9) were cultured with pJA123 and empty pRS426. In both cases, there were small increases in isobutanol titers in the *hxk2Δ* strain compared to WT (Figure

S13, Supporting Information), suggesting a possible correlation between the absence of Hxk2p and increased isobutanol titers, whether through Hxk2p's role in glucose repression[28], extending lifespan[63], or others. Contrary to Y115 however, *hxk2Δ* strain produced similar ethanol levels to WT (Figure S13, Supporting Information). Hence, the absence of Hxk2p alone cannot fully account for the increased isobutanol and decreased ethanol concentrations observed in Y115 compared to WT. Nonetheless, the hexokinase system designed to control glucose flux into glycolysis consistently led to the reduction of ethanol production and improvement in pathway yields from glucose. Even in semi-anaerobic and glucose excess conditions, Y115 reduced ethanol accumulation by 30% and improved isobutanol yields from glucose by more than 3-fold. Additionally, even in cases where isobutanol titers were lower than WT (pJA123 at day 4), isobutanol yields from glucose were still higher in Y115 due to reduced glucose consumption, which is a direct effect of reducing glucose flux with our system. The successful reduction in ethanol production and improvement in isobutanol yields demonstrates the applicability of this system beyond our gluconate model pathway.

Conclusions

We have demonstrated one of the first examples of dynamic glucose redirection away from central carbon metabolism and into a heterologous pathway in *S. cerevisiae*. By integrating the synthetic tTA system into the first step of glycolysis, we developed a genetic valve capable of controlling glycolytic flux. We successfully diverted flux into two different pathways, resulting in significant improvement in yields from glucose. We showed up to a 10-fold decrease in hexokinase activity that allowed the diversion of carbon flux into our model pathway, gluconate, resulting in a 10-fold increase in titers, from 0.15 g/L to 1.8 g/L, and a 50-fold increase in yields, from 0.7% to 36% mol/mol glucose. By varying induction times and inducer concentrations, we obtained strains with different growth rates and gluconate titers, demonstrating the control of glucose flux to either growth or production. In addition, we showed that this system was generalizable in reducing ethanol production in both aerobic and semi-anaerobic conditions, and even in the presence of high external glucose concentrations. Our engineered strain reduced ethanol accumulation by 30% and increased isobutanol yields by more than 3-fold in semi-anaerobic conditions. Although there is additional inducer cost in our current system, this proof-of-concept study shows successful dynamic glucose redirection that resulted in improved yields of heterologous pathways. Further efforts, such as autonomous induction[14,64], may need to be engineered to construct a cost-effective system suitable for production purposes. The success of this study encourages the implementation of other genetic circuits for metabolic control and pathway engineering in *S. cerevisiae*.

Materials and Methods

Strain and Plasmid Construction

S. cerevisiae W303 and CEN.PK2 strains and plasmids used in this study are listed in Table 1. The tetracycline transactivator protein (tTA) system was cloned into the genome from plasmids that were kindly provided by Dr. Narendra Maheshri (MIT Department of Chemical Engineering, Cambridge, MA). Isobutanol overexpression constructs, pJA123 and pJA180[54], were kindly provided by Dr. Gerald Fink (MIT Department of Biology and Whitehead Institute for Biomedical Research, Cambridge, MA). Oligonucleotides used (Table S3) were purchased from Integrated DNA Technologies (Coralville, IA) and Sigma-Genosys (St. Louis, MO). All molecular biology manipulations were carried out according to standard practices[65]. Yeast transformation was performed using standard lithium acetate protocol [66] and mutants were identified and isolated by colony PCR. HXK1 promoter replacement in Y17 was further verified with sequencing. All plasmids were cloned in *E. coli* DH5α using standard chemical transformation [67].

Culture Conditions

Experimental cultures were grown at 30°C in yeast synthetic medium (SD complete) containing Yeast Nitrogen Base (Difco), 2% glucose, and complete amino acids. Gluconate production experiments were performed in SD-leu (lacking leucine). Cultures were grown for 3 days in 50-mL shake flasks with a starting inoculation of OD_{600} 0.01 in the presence of 1000 ng/mL dox. Isobutanol production experiments were performed in SD-ura (lacking uracil) containing 10% glucose, in semi-anaerobic conditions for 10 days in 10-mL tubes. Cultures were grown with a starting inoculation of OD_{600} 0.1 and in the presence of 1000 ng/mL dox for Y115.

Hexokinase Activity Assay

Hexokinase activity assay was performed on crude lysates by resuspending frozen pellets in 750 uL of 10 mM Tris-HCl, 1 mM EDTA, 140 mM NaCl, 0.01% SDS, pH 7.5 and subjected to lysis with glass beads. Supernatant was collected by centrifugation and used as follows. Hexokinase activity was measured in a coupled enzymatic assay[68]. Hexokinase converts glucose to glucose-6-phosphate in the presence of ATP. Glucose-6-phosphate is then converted to 6-phospho-D-gluconate by glucose-6-phosphate dehydrogenase (G6PDH) with the generation of NADPH that is measured on the spectrophotometer at 340 nm. One unit of hexokinase activity will phosphorylate 1.0 μmol/min of D-glucose at pH 7.5 and room temperature in the presence of 3.33 U/mL G6PDH, 60 mM Tris-HCl, 20 mM magnesium chloride, 8.0 mM ATP, 12.0 mM glucose, and 0.9 mM NADP+. Activity measurements were normalized by total protein as measured using the Bradford assay[69].

Metabolite Analysis

Culture supernatant was analyzed on an Agilent 1100 series HPLC instrument with an Aminex HPX-87H column (Bio-Rad Laboratories, Hercules, CA) with 5 mM sulfuric acid as the mobile phase at 35°C and a constant flow rate of 0.6 mL/min. Glucose, ethanol and isobutanol levels were monitored using the refractive index detector (RID) while gluconate was monitored on the diode array detector (DAD) at 230nm. Because glucose and gluconate co-elute at ~9 min on the RID, the DAD signal was used to resolve the two species. Glucose levels were also measured with a YSI 2950D Biochemistry Analyzer (Yellow Springs, OH). Concentrations were determined from standard curves of analytes prepared from Sigma-Aldrich (St. Louis, MO).

Quantification of mRNA levels

Total RNA was extracted from frozen pellets by hot acid chloroform extraction[70]. Briefly, pellets were resuspended in 50 mM sodium acetate pH 5.2 and 10 mM EDTA pH 8. Cells were lysed with the addition of SDS to a final concentration of 1.6% and an equal volume of phenol chloroform isoamyl alcohol. Solutions were heated at 65°C for 10 min and cooled on ice for 5 min. Further extractions were performed with equal volumes of chloroform. RNA was then precipitated with ethanol and resuspended in water. Samples were then treated with TURBO DNase (Life Technologies, Grand Island, NY). Equal amounts of total RNA was then reverse-transcribed using the QuantiTect Reverse Transcription Kit (Qiagen, Valencia, CA) according to manufacturer's instructions. The synthesized cDNA was then amplified with HXK1 specific primers (Table S3) in a qPCR reaction with Brilliant II Sybr Green High ROX QPCR Mix (Agilent Technologies, Santa Clara, CA) on an ABI 7300 Real Time PCR System instrument (Applied Biosystems, Beverly, MA). Transcript levels were quantified in duplicate with appropriate no-template, no-RT and serial dilution controls. Reported levels are the averages of biological triplicates, each measured in technical duplicates.

Supporting Information

Additional methods, figures and tables.

Author information

Corresponding author

Email: kljp@mit.edu

Acknowledgments

This work was funded by the National Institute of General Medical Sciences (NIGMS), Grant P50 GM098792.

References

(1) Ro, D.-K., Paradise, E. M., Ouellet, M., Fisher, K. J., Newman, K. L., Ndungu, J. M., Ho, K. a, Eachus, R. a, Ham, T. S., Kirby, J., Chang, M. C. Y., Withers, S. T., Shiba, Y., Sarpong, R., and Keasling, J. D. (2006) Production of the antimalarial drug precursor artemisinic acid in engineered yeast. *Nature 440*, 940–3.

(2) Kunjapur, A. M., Tarasova, Y., and Prather, K. L. J. (2014) Synthesis and Accumulation of Aromatic Aldehydes in an Engineered Strain of *Escherichia coli*. *J. Am. Chem. Soc. 136*, 11644–54.

(3) Wei, N., Quarterman, J., Kim, S. R., Cate, J. H. D., and Jin, Y.-S. (2013) Enhanced biofuel production through coupled acetic acid and xylose consumption by engineered yeast. *Nat. Commun. 4*.

(4) Shimada, H., Kondo, K., Fraser, P. D., Miura, Y., Saito, T., and Misawa, N. (1998) Increased carotenoid production by the food yeast *Candida utilis* through metabolic engineering of the isoprenoid pathway. *Appl. Environ. Microbiol. 64*, 2676–2680.

(5) Ostergaard, S., Olsson, L., Johnston, M., and Nielsen, J. (2000) Increasing galactose consumption by *Saccharomyces cerevisiae* through metabolic engineering of the GAL gene regulatory network. *Nat. Biotechnol. 18*, 1283–6.

(6) Watanabe, S., Abu Saleh, A., Pack, S. P., Annaluru, N., Kodaki, T., and Makino, K. (2007) Ethanol production from xylose by recombinant *Saccharomyces cerevisiae* expressing protein-engineered NADH-preferring xylose reductase from *Pichia stipitis*. *Microbiology 153*, 3044–54.

(7) Solomon, K. V, and Prather, K. L. J. (2011) The zero-sum game of pathway optimization: emerging paradigms for tuning gene expression. *Biotechnol. J. 6*, 1064–70.

(8) Glick, B. R. (1995) Metabolic load and heterologous gene expression. *Biotechnol. Adv. 13*, 247–261.

(9) Holtz, W. J., and Keasling, J. D. (2010) Engineering static and dynamic control of synthetic pathways. *Cell 140*, 19–23.

(10) Gilbert, L. a, Larson, M. H., Morsut, L., Liu, Z., Brar, G. a, Torres, S. E., Stern-Ginossar, N., Brandman, O., Whitehead, E. H., Doudna, J. a, Lim, W. a, Weissman, J. S., and Qi, L. S. (2013) CRISPR-mediated modular RNA-guided regulation of transcription in eukaryotes. *Cell 154*, 442–51.

(11) Shong, J., and Collins, C. H. (2013) Engineering the esaR promoter for tunable quorum sensing- dependent gene expression. *ACS Synth. Biol. 2*, 568–75.

(12) Solomon, K. V, Sanders, T. M., and Prather, K. L. J. (2012) A dynamic metabolite valve for the control of central carbon metabolism. *Metab. Eng. 14*, 661–71.

(13) Brockman, I. M., and Prather, K. L. J. (2014) Dynamic knockdown of *E. coli* central metabolism for redirecting fluxes of primary metabolites. *Metab. Eng. 28*, 104–113.

(14) Xu, P., Li, L., Zhang, F., Stephanopoulos, G., and Koffas, M. (2014) Improving fatty acids production by engineering dynamic pathway regulation and metabolic control. *Proc. Natl. Acad. Sci. 111*, 1–6.

(15) Xu, P., Gu, Q., Wang, W., Wong, L., Bower, A. G. W., Collins, C. H., and Koffas, M. A. G. (2013) Modular optimization of multi-gene pathways for fatty acids production in *E. coli*. *Nat. Commun. 4*, 1409.

(16) Soma, Y., Tsuruno, K., Wada, M., Yokota, A., and Hanai, T. (2014) Metabolic flux redirection from a central metabolic pathway toward a synthetic pathway using a metabolic toggle switch. *Metab. Eng. 23*, 175–84.

(17) Asadollahi, M. a, Maury, J., Schalk, M., Clark, A., and Nielsen, J. (2010) Enhancement of farnesyl diphosphate pool as direct precursor of sesquiterpenes through metabolic engineering of the mevalonate pathway in *Saccharomyces cerevisiae*. *Biotechnol. Bioeng. 106*, 86–96.

(18) Paradise, E. M., Kirby, J., Chan, R., and Keasling, J. D. (2008) Redirection of flux through the FPP branch-point in *Saccharomyces cerevisiae* by down-regulating squalene synthase. *Biotechnol. Bioeng. 100*, 371–8.

(19) Scalcinati, G., Knuf, C., Partow, S., Chen, Y., Maury, J., Schalk, M., Daviet, L., Nielsen, J., and Siewers, V. (2012) Dynamic control of gene expression in *Saccharomyces cerevisiae* engineered for the production of plant sesquitepene α-santalene in a fed-batch mode. *Metab. Eng. 14*, 91–103.

(20) Yamanishi, M., and Matsuyama, T. (2012) A modified Cre-lox genetic switch to dynamically control metabolic flow in *Saccharomyces cerevisiae*. *ACS Synth. Biol. 1*, 172–80.

(21) Møller, K., Nielsen, K. F., Asadollahi, M. A., Schalk, M., Clark, A., and Nielsen, J. (2008) Production of Plant Sesquiterpenes in *Saccharomyces cerevisiae* : Effect of ERG9 Repression on Sesquiterpene Biosynthesis *99*, 666–677.

(22) Polakis, E. S., and Bartley, W. (1965) Changes in the enzyme activities of *Saccharomyces cerevisiae* during aerobic growth on different carbon sources. *Biochem. J. 97*, 284.

(23) Umemura, K., Atomi, H., Kanai, T., Teranishi, Y., Ueda, M., and Tanaka, A. (1995) Effects of carbon source on the application of a novel foreign gene expression system in *Saccharomyces cerevisiae* using the upstream region of the *Candida tropicalis* isocitrate lyase gene (UPR-ICL). *J. Ferment. Bioeng. 80*, 529–533.

(24) Williams, T. C., Averesch, N. J. H., Winter, G., Plan, M. R., Vickers, C. E., Nielsen, L. K., and Krömer, J. O. (2015) Quorum-sensing linked RNA interference for dynamic metabolic

pathway control in *Saccharomyces cerevisiae*. *Metab. Eng. 29*, 124–134.

(25) Yuan, J., and Ching, C. B. (2015) Dynamic control of ERG9 expression for improved amorpha-4,11-diene production in *Saccharomyces cerevisiae*. *Microb. Cell Fact. 14*.

(26) Trumbly, R. J. (1992) Glucose repression in the yeast *Saccharomyces cerevisiae*. *Mol. Microbiol. 6*, 15–21.

(27) Vemuri, G. N., Eiteman, M. a, McEwen, J. E., Olsson, L., and Nielsen, J. (2007) Increasing NADH oxidation reduces overflow metabolism in *Saccharomyces cerevisiae*. *Proc. Natl. Acad. Sci. U. S. A. 104*, 2402–7.

(28) Broach, J. R. (2012) Nutritional control of growth and development in yeast. *Genetics 192*, 73–105.

(29) Herrero, P., Galíndez, J., Ruiz, N., Martínez-Campa, C., and Moreno, F. (1995) Transcriptional regulation of the *Saccharomyces cerevisiae* HXK1, HXK2 and GLK1 genes. *Yeast 11*, 137–44.

(30) Garí, E., Piedrafita, L., Aldea, M., and Herrero, E. (1997) A set of vectors with a tetracycline-regulatable promoter system for modulated gene expression in *Saccharomyces cerevisiae*. *Yeast 13*, 837–48.

(31) Ramachandran, S., Fontanille, P., Pandey, A., and Larroche, C. (2006) Gluconic Acid: Properties, Applications and Microbial Production *44*, 185–195.

(32) Anastassiadis, S., and Morgunov, I. (2007) Gluconic Acid Production. *Recent Pat. Biotechnol. 1*, 167–180.

(33) Anastassiadis, S., and Rehm, H.-J. (2006) Continuous gluconic acid production by *Aureobasidium pullulans* with and without biomass retention. *Electron. J. Biotechnol. 9*.

(34) Ramaley, R., and Vasantha, N. (1983) Glycerol protection and purification of *Bacillus subtilis* glucose dehydrogenase. *J. Biol. Chem. 258*, 12558–12565.

(35) Gao, H., and Leary, J. A. (2003) Multiplex inhibitor screening and kinetic constant determinations for yeast hexokinase using mass spectrometry based assays. *J. Am. Soc. Mass Spectrom. 14*, 173–81.

(36) Fernandez, R., Herrero, P., and Moreno, F. (1985) Inhibition and Inactivation of Glucose-phosphorylating Enzymes from *Saccharomyces cerevisiae* by D-Xylose. *Microbiology 131*, 2705–2709.

(37) Rodriguez, A., de la Cera, T., Herrero, P., and Moreno, F. (2001) The hexokinase 2 protein regulates the expression of the GLK1, HXK1 and HXK2 genes of *Saccharomyces cerevisiae*. *Biochem. J. 355*, 625–631.

(38) Bellí, G., Garí, E., Piedrafita, L., Aldea, M., and Herrero, E. (1998) An activator/repressor dual system allows tight tetracycline-regulated gene expression in budding yeast. *Nucleic Acids Res. 26*, 942–7.

(39) Raamsdonk, O. M., Kruckeberg, A. L., Diderich, J. A., Berden, J. A. N. A., and Dam, K. V. A. N. (2001) Physiological Properties of *Saccharomyces cerevisiae* from Which Hexokinase II Has Been Deleted *67*, 1587–1593.

(40) Gygi, S. P., Rochon, Y., Franza, B. R., and Aebersold, R. (1999) Correlation between Protein and mRNA Abundance in Yeast. *Mol. Cell. Biol. 19*, 1720–1730.

(41) Belle, A., Tanay, A., Bitincka, L., Shamir, R., and O'Shea, E. K. (2006) Quantification of protein half-lives in the budding yeast proteome. *Proc. Natl. Acad. Sci. U. S. A. 103*, 13004–9.

(42) Daran-Lapujade, P., Rossell, S., van Gulik, W. M., Luttik, M. a H., de Groot, M. J. L., Slijper, M., Heck, A. J. R., Daran, J.-M., de Winde, J. H., Westerhoff, H. V, Pronk, J. T., and Bakker, B. M. (2007) The fluxes through glycolytic enzymes in *Saccharomyces cerevisiae* are predominantly regulated at posttranscriptional levels. *Proc. Natl. Acad. Sci. U. S. A. 104*, 15753–8.

(43) Lacroute, F. (1973) RNA and protein elongation rates in *Saccharomyces cerevisiae*. *Mol. Gen. Genet. MGG 125*, 319–327.

(44) Miller, C., Schwalb, B., Maier, K., Schulz, D., Dümcke, S., Zacher, B., Mayer, A., Sydow, J., Marcinowski, L., Dölken, L., Martin, D. E., Tresch, A., and Cramer, P. (2011) Dynamic transcriptome analysis measures rates of mRNA synthesis and decay in yeast. *Mol. Syst. Biol. 7*, 458.

(45) Van Hoek, P., Van Dijken, J. P., and Pronk, J. T. (1998) Effect of specific growth rate on fermentative capacity of baker's yeast. *Appl. Environ. Microbiol. 64*, 4226–33.

(46) Diderich, J. a., Schepper, M., van Hoek, P., Luttik, M. a. H., van Dijken, J. P., Pronk, J. T., Klaassen, P., Boelens, H. F. M., de Mattos, M. J. T., van Dam, K., and Kruckeberg, a. L. (1999) Glucose Uptake Kinetics and Transcription of HXT Genes in Chemostat Cultures of *Saccharomyces cerevisiae*. *J. Biol. Chem. 274*, 15350–15359.

(47) Ozcan, S., and Johnston, M. (1999) Function and regulation of yeast hexose transporters. *Microbiol. Mol. Biol. Rev. 63*, 554–69.

(48) Postma, E., Scheffers, W. a, and van Dijken, J. P. (2000) Kinetics of growth and glucose transport in glucose-limited chemostat cultures of *Saccharomyces cerevisiae* CBS 8066. *Yeast 5*, 159–65.

(49) Otterstedt, K., Larsson, C., Bill, R. M., Ståhlberg, A., Boles, E., Hohmann, S., and Gustafsson, L. (2004) Switching the mode of metabolism in the yeast *Saccharomyces cerevisiae*.

EMBO Rep. 5, 532–7.

(50) Hazelwood, L. a, Daran, J.-M., van Maris, A. J. a, Pronk, J. T., and Dickinson, J. R. (2008) The Ehrlich pathway for fusel alcohol production: a century of research on *Saccharomyces cerevisiae* metabolism. *Appl. Environ. Microbiol. 74*, 2259–66.

(51) Chen, X., Nielsen, K. F., Borodina, I., Kielland-Brandt, M. C., and Karhumaa, K. (2011) Increased isobutanol production in *Saccharomyces cerevisiae* by overexpression of genes in valine metabolism. *Biotechnol. Biofuels 4*, 21.

(52) Matsuda, F., Ishii, J., Kondo, T., Ida, K., Tezuka, H., and Kondo, A. (2013) Increased isobutanol production in *Saccharomyces cerevisiae* by eliminating competing pathways and resolving cofactor imbalance. *Microb. Cell Fact. 12*, 119.

(53) Ida, K., Ishii, J., Matsuda, F., Kondo, T., and Kondo, A. (2015) Eliminating the isoleucine biosynthetic pathway to reduce competitive carbon outflow during isobutanol production by *Saccharomyces cerevisiae*. *Microb. Cell Fact. 14*, 1–9.

(54) Avalos, J. L., Fink, G. R., and Stephanopoulos, G. (2013) Compartmentalization of metabolic pathways in yeast mitochondria improves the production of branched-chain alcohols. *Nat. Biotechnol. 31*, 335–41.

(55) Brat, D., Weber, C., Lorenzen, W., Bode, H. B., and Boles, E. (2012) Cytosolic re-localization and optimization of valine synthesis and catabolism enables inseased isobutanol production with the yeast *Saccharomyces cerevisiae*. *Biotechnol. Biofuels 5*, 65.

(56) Kondo, T., Tezuka, H., Ishii, J., Matsuda, F., Ogino, C., and Kondo, A. (2012) Genetic engineering to enhance the Ehrlich pathway and alter carbon flux for increased isobutanol production from glucose by *Saccharomyces cerevisiae*. *J. Biotechnol. 159*, 32–7.

(57) Bai, F. W., Chen, L. J., Zhang, Z., Anderson, W. a., and Moo-Young, M. (2004) Continuous ethanol production and evaluation of yeast cell lysis and viability loss under very high gravity medium conditions. *J. Biotechnol. 110*, 287–293.

(58) Flikweert, M. T., Van der Zanden, L., Janssen, W., Steensma, H. Y. D. E., van Dijken, J. P., and Pronk, J. T. (1996) Pyruvate Decarboxylase: An Indispensable Enzyme for Growth of *Saccharomyces cerevisiae* on Glucose. *Yeast 12*, 247–257.

(59) Flikweert, M. T., Swaaf, M. De, Dijken, J. P. Van, and Pronk, J. T. (1999) Growth requirements of pyruvate-decarboxylase-negative *Saccharomyces cerevisiae 174*, 73–79.

(60) Natarajan, K., Meyer, M. R., Belinda, M., Slade, D., Roberts, C., Alan, G., Marton, M. J., Jackson, B. M., and Hinnebusch, A. G. (2001) Transcriptional Profiling Shows that Gcn4p Is a Master Regulator of Gene Expression during Amino Acid Starvation in Yeast. *Mol. Cell. Biol. 21*, 4347–4368.

(61) Arndt, K., and Fink, G. R. (1986) GCN4 protein, a positive transcription factor in yeast, binds general control promoters at all 5’ TGACTC 3' sequences. *Proc. Natl. Acad. Sci. U. S. A. 83*, 8516–8520.

(62) Albrecht, G., Mösch, H., Reusser, U., Gerhard, H., Chem, J. B., Mo, H., Hoffmann, B., and Braus, G. H. (1998) Monitoring the Gcn4 Protein-mediated Response in the Yeast *Saccharomyces cerevisiae*. *J. Biol. Chem. 273*, 12696–12702.

(63) Lin, S. J., Defossez, P. a, and Guarente, L. (2000) Requirement of NAD and SIR2 for life-span extension by calorie restriction in *Saccharomyces cerevisiae*. *Science 289*, 2126–2128.

(64) Zhang, F., Carothers, J. M., and Keasling, J. D. (2012) Design of a dynamic sensor-regulator system for production of chemicals and fuels derived from fatty acids. *Nat. Biotechnol. 30*, 354–9.

(65) Green, M. R., and Sambrook, J. (2012) Molecular Cloning: A Laboratory Manual Fourth. Cold Spring Harbor Laboratory Press, Cold Spring Harbor, NY.

(66) Kawai, S., Hashimoto, W., and Murata, K. Transformation of *Saccharomyces cerevisiae* and other fungi: methods and possible underlying mechanism. *Bioeng. Bugs 1*, 395–403.

(67) Hanahan, D., Jessee, J., and Bloom, F. R. (1991) Plasmid transformation of *Escherichia coli* and other bacteria. *Methods Enzymol. 204*, 63–113.

(68) Dipierto, D. L., and Weinhouse, S. (1960) Hepatic glucokinase in the fed, fasted, and alloxan-diabetic rat. *J. Biol. Chem. 235*, 2542–5.

(69) Zor, T., and Selinger, Z. (1996) Linearization of the Bradford protein assay increases its sensitivity: theoretical and experimental studies. *Anal. Biochem. 236*, 302–8.

(70) Ares, M. (2012) Isolation of total RNA from yeast cell cultures. *Cold Spring Harb. Protoc. 2012*, 1082–6.

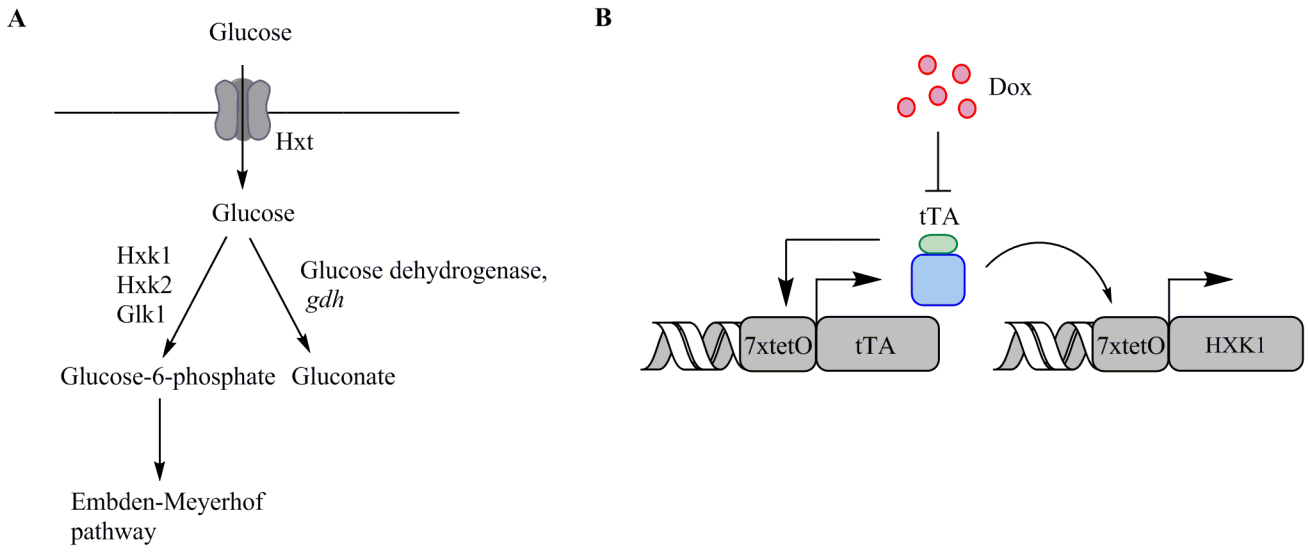

Figure 1. Glucose valve construction. (A) In a *hxk2Δ glk1Δ* strain, a glucose valve was constructed by controlling the transcription of Hxk1p in order to divert flux into the gluconate pathway. (B) The tTA protein, which consists of TetR fused to a VP16 activating domain, was expressed with 7xtetO CYC1 TATA from the TRP1 locus. The native HXK1 promoter was also replaced with 7xtetO CYC1 TATA. Upon addition of doxycycline (Dox), the binding of Dox to tTA causes a conformational change that releases tTA from the DNA, thereby repressing transcription of HXK1.

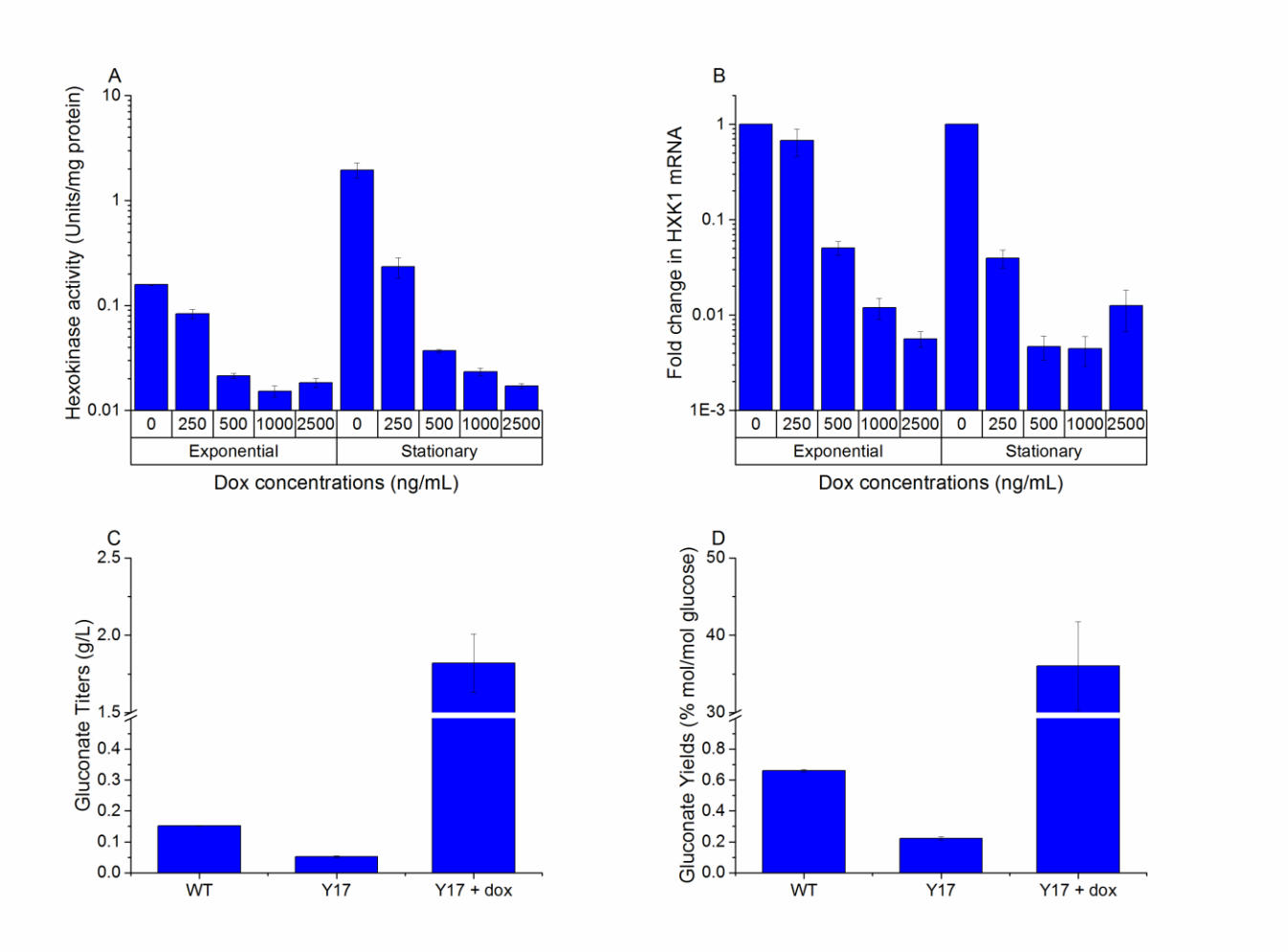

Figure 2. Characterization of glucose valve and improvement in gluconate titers and yields. (A) Addition of doxycycline represses hexokinase activity in a dose dependent manner, as measured in cell lysate at late exponential and stationary phase. (B) Fold change in HXK1 mRNA of strains in (A) compared to un-induced (0 ng/mL dox) condition, as measured at late exponential and stationary phase. (C) Gluconate titers (g/L) and (D) gluconate yields (% mol/mol glucose) of WT and Y17, with and without 1000 ng/mL dox induction. Error bars represent standard error among three biological replicates.

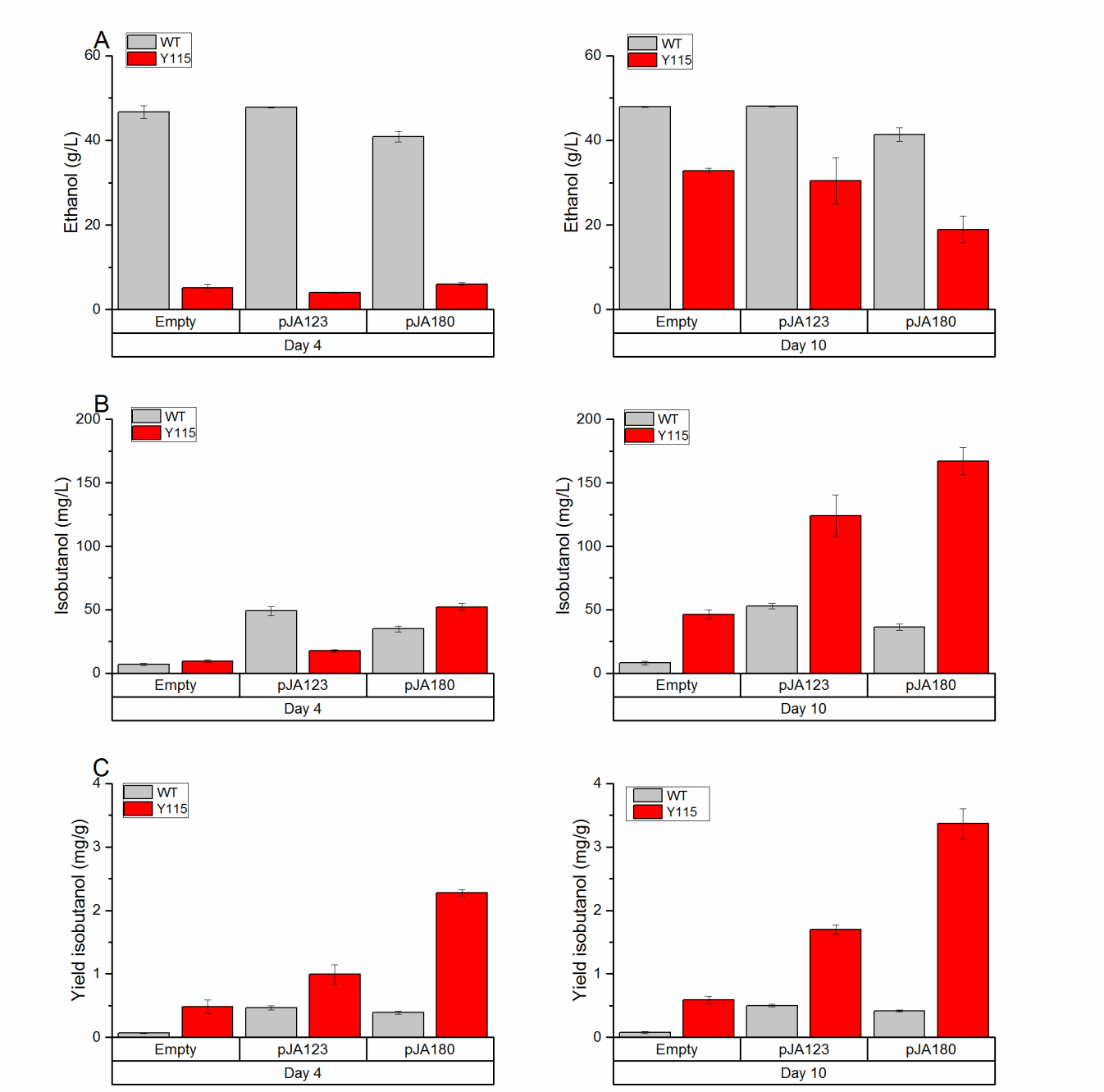

Figure 3. Improvement in isobutanol titers and yields. (A) Ethanol production (g/L) of WT and Y115 at day 4 and day 10. (B) Isobutanol titers (mg/L) and (C) yields (mg/g glucose) of WT and Y115 at day 4 and day 10. Error bars represent standard error among three biological replicates.

Table 1. Genotype of (A) strains and (B) plasmids used in this study.

Table 1(A)

Strain	Parent	Genetic change	Reference/Source
W303	N/A	MATa**;** ura3-1; leu2-3; 112 trp1-1; his3-11, 5; can1-100; ade2-1; GAL^{+}	
WT	W303	ura3::URA3, trp1::TRP1, his3::HIS3, leu2Δ::7xtetO YFP	This study
Y9	W303	hxk2::CgHIS3	This study
Y12	W303	glk1::KanMX, hxk2::CgHIS3	This study
Y15	Y12	trp1::7xtetO tTA	This study
Y17	Y15	HXK1 pr::7xtetO CYC1 TATA klURA3	This study
CEN.PK2-1D	N/A	MATα; ura3-52; trp1-289; leu2-3,112; his3Δ 1; $MAL2\text{-}8^{C}$; SUC2	EUROSCARF
WT	CEN.PK2-1D	ura3::URA3, trp1::TRP1, his3::HIS3	This study
Y115	CEN.PK2-1D	glk1::KanMX, hxk2::CgHIS3, trp1::7xtetO tTA, HXK1 pr::7xtetO CYC1 TATA	This study

Table 1(B)

Plasmid	Genotype	Reference/Source
pRS304 7xtetO tTA	7xtetO CYC1 TATA tTA	This study
pRS415-*gdh*	P_{ADH1} *B.subtilis gdh*	This study
pRS415	Empty control for gluconate experiments	
pRS415 7xtetO YFP	7xtetO CYC1 TATA YFP	This study
pJA 123	P_{TDH3}ScILV2, P_{PGK1} ScILV3, P_{TEF1} ScILV5	(54)
pJA 180	P_{TDH3}ScILV2, P_{PGK1} ScILV3, P_{TEF1} ScILV5, P_{TDH3}CoxIV-LlKivd, P_{TEF1}CoxIV-LlAdhA(RE1)	(54)
pRS426	Empty control for isobutanol experiments	

For Table of Contents Use only

Controlling Central Carbon Metabolism for Improved Pathway Yields in *Saccharomyces cerevisiae*

Sue Zanne Tan, Shawn Manchester and Kristala L. J. Prather

Table of Contents Graphic

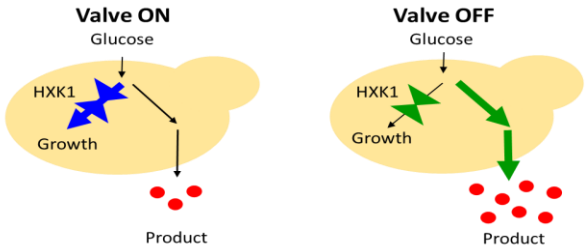

Supporting Information

Controlling Central Carbon Metabolism for Improved Pathway Yields in *Saccharomyces cerevisiae*

Sue Zanne Tan, Shawn Manchester and Kristala L. J. Prather

MATLAB simulation parameters

The following equations were used to illustrate the magnitude of growth-mediated buffering effect on changes in mRNA abundance.

mRNA, *m*, balance:

$$\frac{dm}{dt} = \alpha - (k_d + \mu)m$$

Where α = mRNA transcription rate, k_d = mRNA decay rate, and μ = growth rate.

Protein, *p*, balance:

$$\frac{dp}{dt} = \beta m - \mu p$$

Where β = translation rate.

The growth rate, μ, was estimated by

$$\mu = \gamma p + \varphi$$

Where γ and φ were estimated by the slope and intercept of experimentally obtained growth rate vs. hexokinase activity. $\gamma = 0.0705\ hr^{-1}$ and $\varphi = 0.0436 \frac{U}{mg.hr}$

The following parameters were used in the simulation:

HXK1 transcription rate, α = 0.00653 molecules/cell/min [1]

HXK1 mRNA decay rate, k_d = 0.02 min^{-1} [1]

Turnover of Hxk1p, k_{cat} = 1.06 s^{-1} [2]

Mass of protein/cell in *S. cerevisiae* = 4×10^{-12} g [3]

Continuous stirred tank reactor culture of WT pJA123

Continuous stirred tank reactor cultures of WT pJA123 were performed in SD ura- containing 10% glucose to mimic conditions in batch experiments, in semi-anaerobic conditions in 50mL Wheaton Celstir Spinner Double Side Arm flasks. Fresh media was constantly flowed into the reactor at the same rate as the outlet flow of cells, using Masterflex pumps. Dilution rates achieved were 0.027, 0.03, 0.046, 0.063, 0.055, 0.053, 0.12 and 0.12 hr^{-1}, calculated by measuring inlet flow rates. Samples were taken at steady state and after >5 volumes of reactor have passed.

Glucose dehydrogenase Activity Assay

Glucose dehydrogenase activity was measured directly from the oxidation of glucose to gluconic acid with the production of NADH. One unit of Gdh activity oxidizes 1.0 μmol/min of D-glucose at pH 7.6 at room temperature in 60 mM potassium phosphate buffer and 0.67 mM NAD+.

AHAS Activity Assay

AHAS activity was measured by the colorimetric single-point method [4]. The optimized assay contained 50mM sodium pyruvate, 1mM thiamine pyrophosphate, 10mM $MgCl_2$, 10μM FAD, and 7.2mM ATP in 1.15M potassium phosphate buffer pH 7.0. Cell lysates were prepared using Y-PER Yeast Protein Extraction Reagent (Life Technologies, Grand Island, NY) and incubated in 5 mg/mL lyticase (Sigma Aldrich, St. Louis, MO) at 30°C for 30min. Equal volumes of cell lysate and assay mix were then incubated at 30°C for 20min and the reaction was stopped by the addition of 50% H_2SO_4 to a final concentration of 1%. After incubation at 60°C for 15min to convert acetolactate to acetoin, acetoin was then quantified by further incubation at 30°C for 10min in the presence of 0.15% creatine and freshly prepared 1.5% α-naphthol (in 2.5N NaOH). The color developed was measured at 540nm and acetoin was used as a standard. One unit (U) of activity is defined as that producing 1 μmol of 2-acetolactate per minute under the above conditions. Protein concentrations were measured using the BCA kit (Thermo Scientific, Grand Island, NY).

References

(1) Miller, C., Schwalb, B., Maier, K., Schulz, D., Dümcke, S., Zacher, B., Mayer, A., Sydow, J., Marcinowski, L., Dölken, L., Martin, D. E., Tresch, A., and Cramer, P. (2011) Dynamic transcriptome analysis measures rates of mRNA synthesis and decay in yeast. *Mol. Syst. Biol. 7*, 458.

(2) Gao, H., and Leary, J. A. (2003) Multiplex inhibitor screening and kinetic constant determinations for yeast hexokinase using mass spectrometry based assays. *J. Am. Soc. Mass Spectrom. 14*, 173–81.

(3) Futcher, B., Latter, G. I., Monardo, P., Mclaughlin, C. S., Garrels, I., and Laughlin, C. S. M. C. (1999) A Sampling of the Yeast Proteome These include : A Sampling of the Yeast Proteome *19*.

(4) Pang, S. S., and Duggleby, R. G. (2001) Regulation of yeast acetohydroxyacid synthase by valine and ATP. *Biochem. J.* 749–757.

(5) McCartney, R. R., and Schmidt, M. C. (2001) Regulation of Snf1 Kinase. Activation requires phosphorylation of threonine 210 by an upstream kinase as well as a distinct step mediated by the Snf4 subunit. *J. Biol. Chem. 276*, 36460–36466.

(6) Shirra, M. K., McCartney, R. R., Zhang, C., Shokat, K. M., Schmidt, M. C., and Arndt, K. M. (2008) A chemical genomics study identifies Snf1 as a repressor of GCN4 translation. *J. Biol. Chem. 283*, 35889–35898.

(7) Natarajan, K., Meyer, M. R., Belinda, M., Slade, D., Roberts, C., Alan, G., Marton, M. J., Jackson, B. M., and Hinnebusch, A. G. (2001) Transcriptional Profiling Shows that Gcn4p Is a Master Regulator of Gene Expression during Amino Acid Starvation in Yeast Transcriptional Profiling Shows that Gcn4p Is a Master Regulator of Gene Expression during Amino Acid Starvation in Yeast. *Mol. Cell. Biol. 21*, 4347–4368.

(8) Arndt, K., and Fink, G. R. (1986) GCN4 protein, a positive transcription factor in yeast, binds general control promoters at all 5’ TGACTC 3' sequences. *Proc. Natl. Acad. Sci. U. S. A. 83*, 8516–8520.

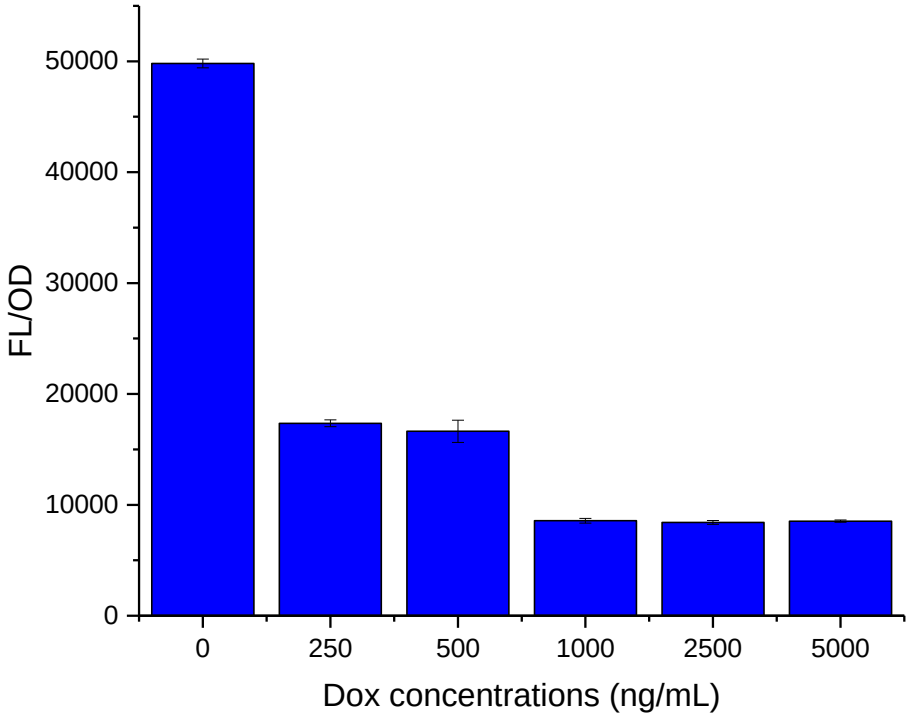

Figure S1. YFP fluorescence (normalized by OD_{600}) of cells expressing 7xtetO tTA from the genome and PRS415 7xtetO YFP, with increasing dox concentrations (ng/mL). Dox addition was performed at inoculation, OD_{600} 0.1. Error bars represent standard error among three biological replicates.

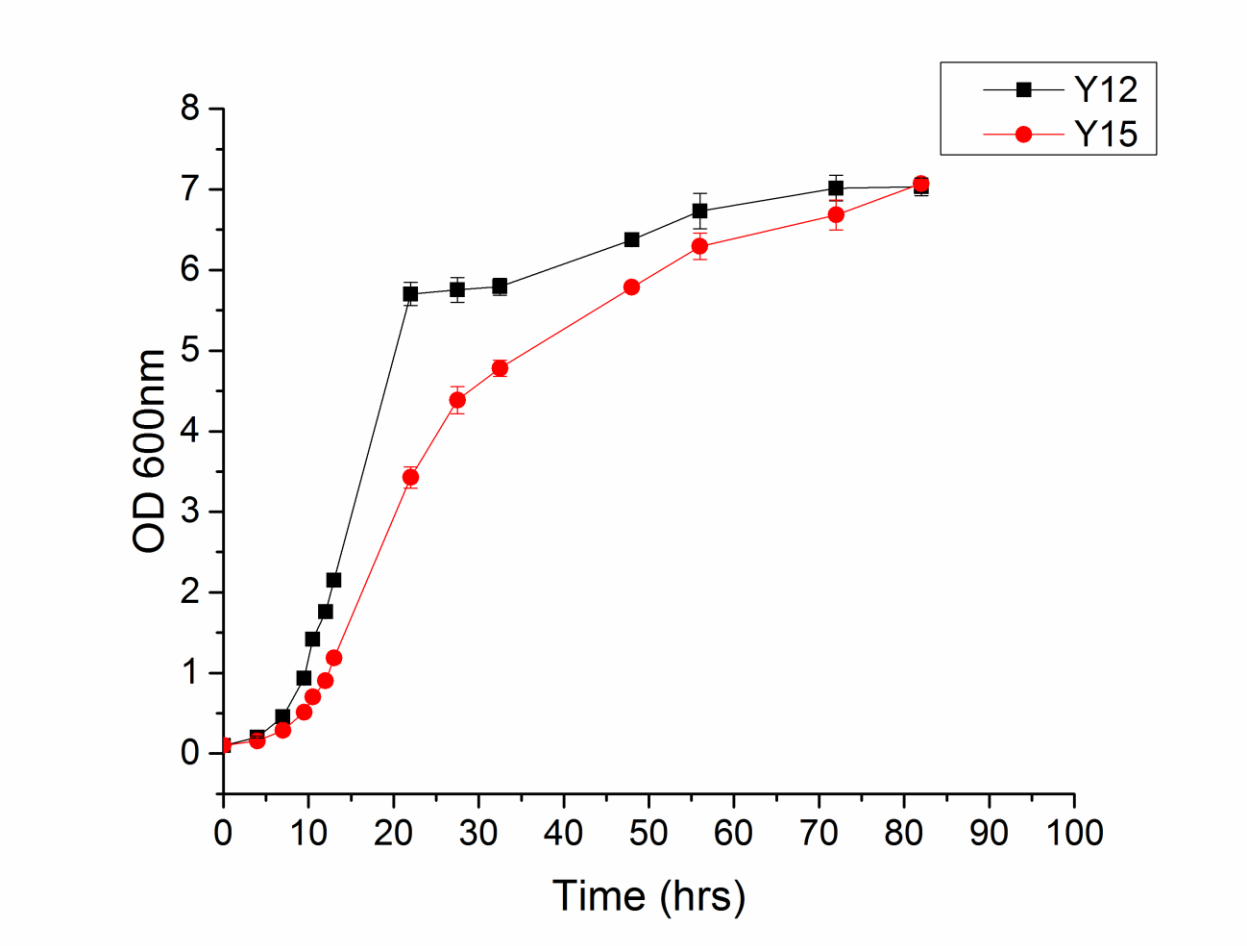

Figure S2: Growth curve of strain Y15 expressing tTA (*hxk2Δ glk1Δ* trp1::7xtetO tTA) compared to Y12 (*hxk2Δ glk1Δ*). Error bars represent standard error among three biological replicates.

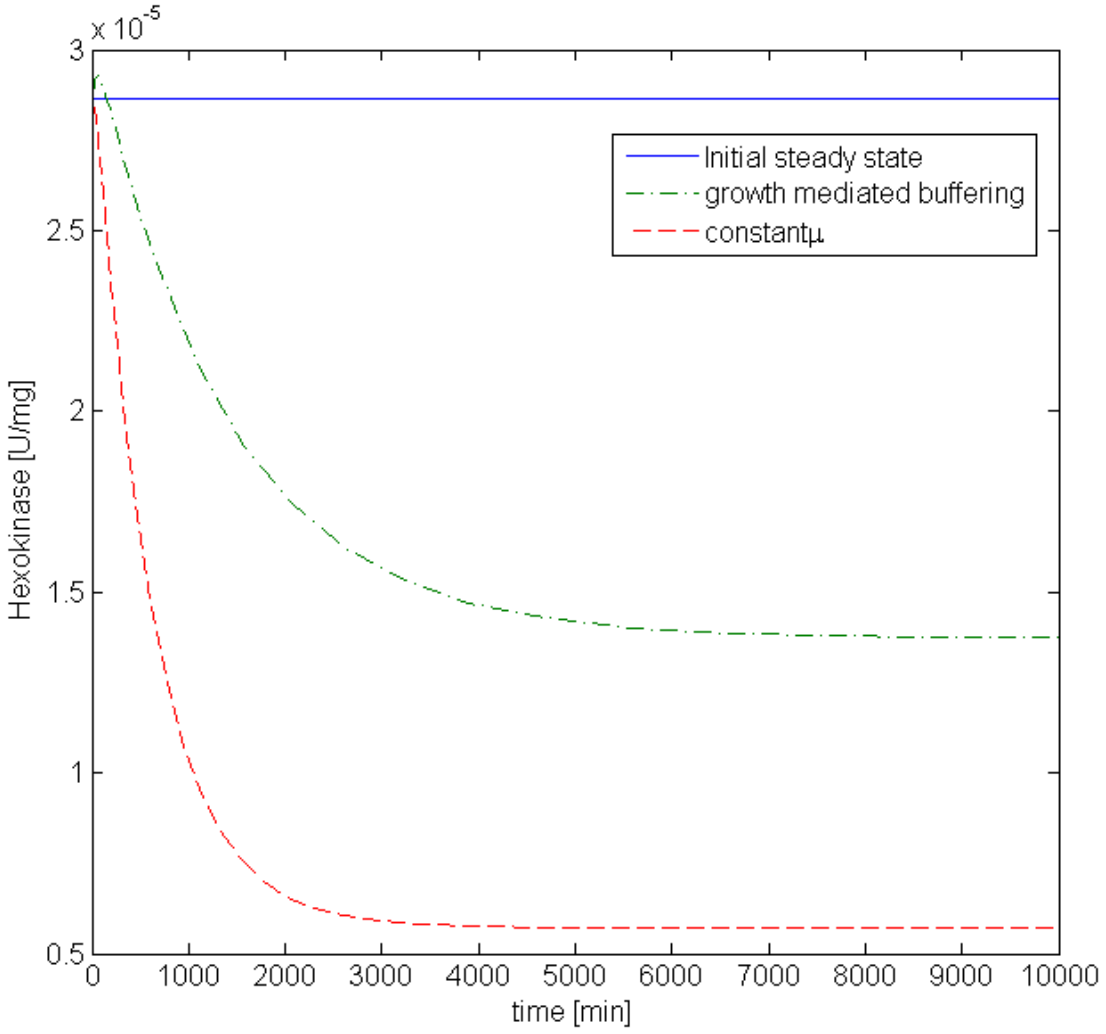

Figure S3. MATLAB simulation of hexokinase activity (U/mg) as a result of an 80% reduction in mRNA synthesis rate, for a constant growth assumption and with growth mediated buffering effects.

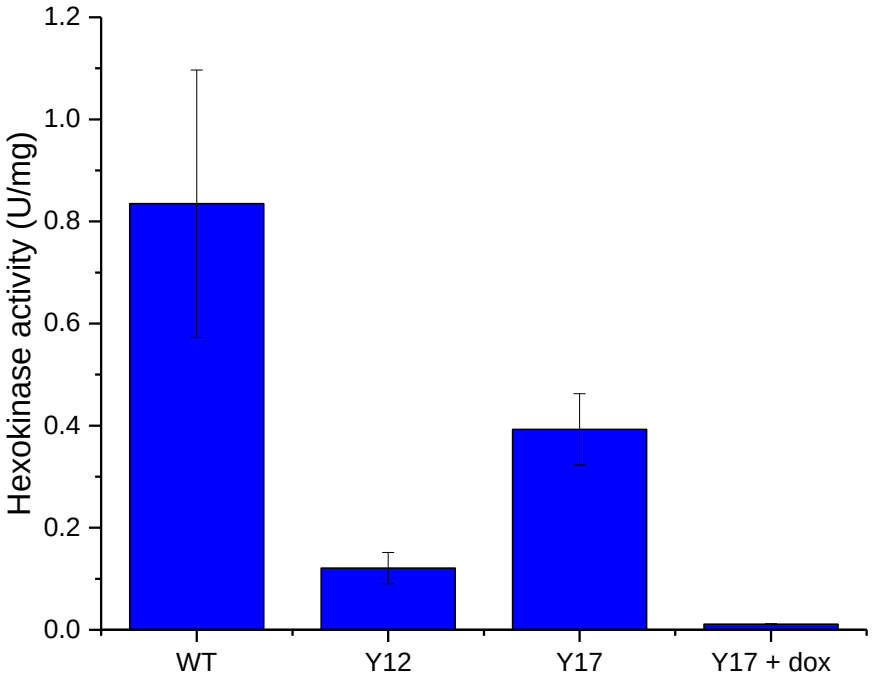

Figure S4. Hexokinase activity (U/mg protein), as measured in cell lysates at late-exponential phase, of WT, Y12, Y17 and Y17+dox strains. Error bars represent standard error among three biological replicates.

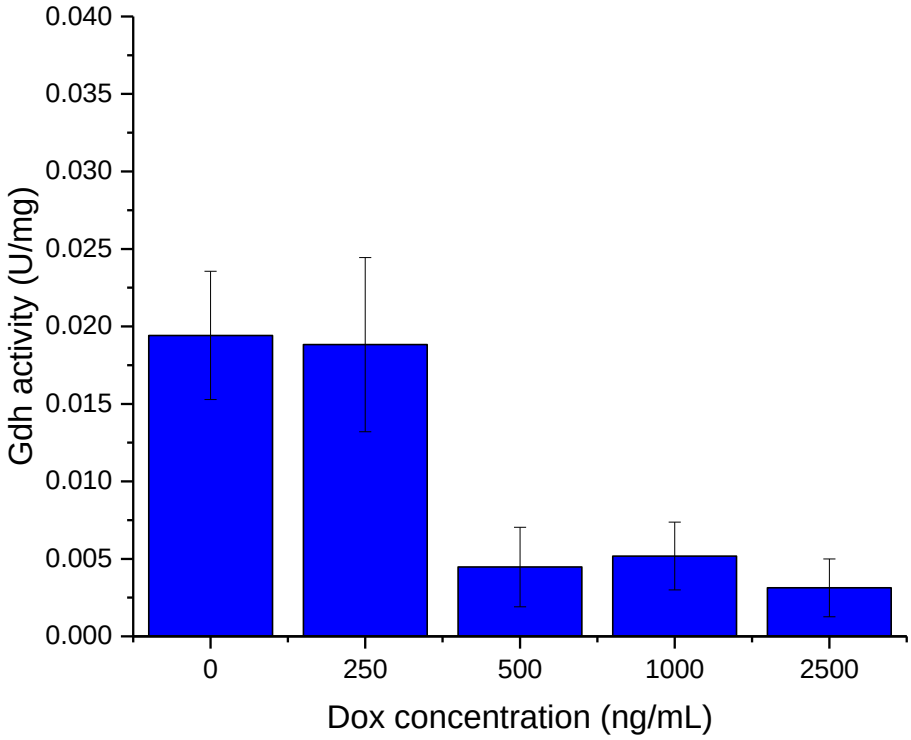

Figure S5. Glucose dehydrogenase, Gdh, activity (U/mg protein), as measured in cell lysates at stationary phase, of Y17 at different dox concentrations (ng/mL). Error bars represent standard error among three biological replicates.

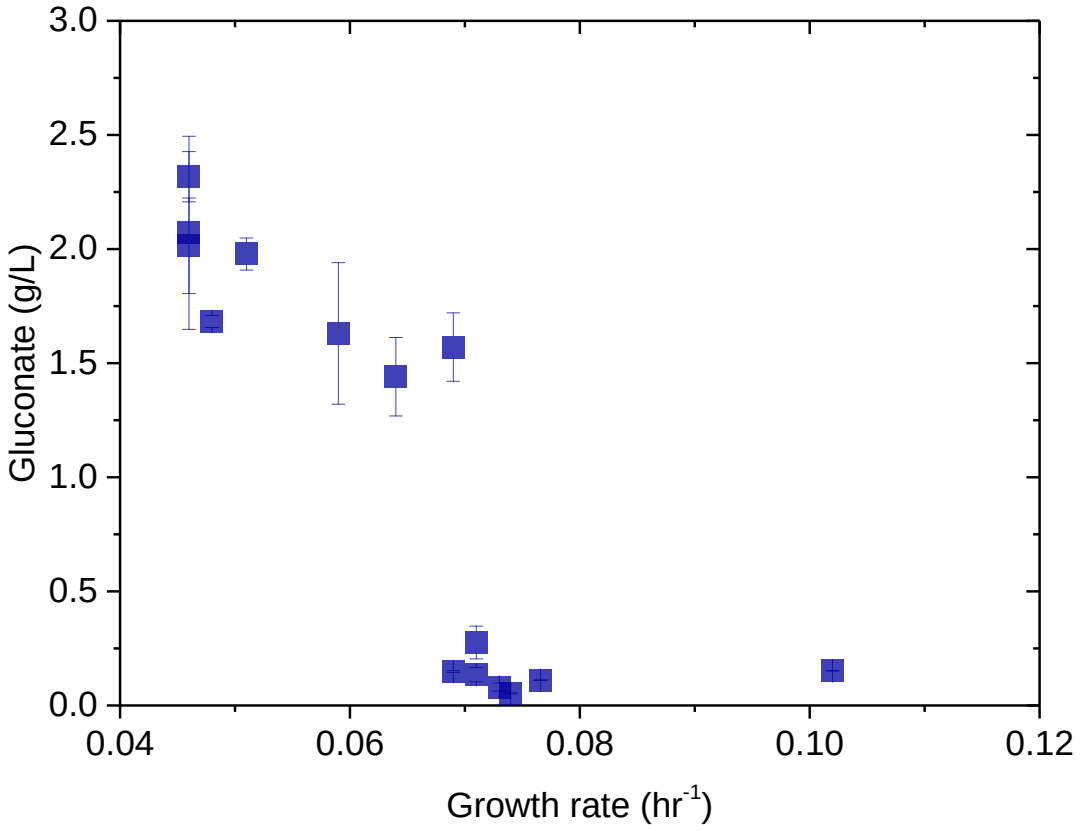

Figure S6. Gluconate titers (g/L) of Y17 strains at different growth rates (1/hr), achieved by varying amounts of dox concentration and induction time, as shown in Table S1. Each data point represents a biological triplicate of an experiment performed at a specific dox concentration, from 0 to 2500 ng/mL, and timing of induction, from OD_{600} 0.01 to OD_{600} 1. Error bars represent standard error among three biological replicates.

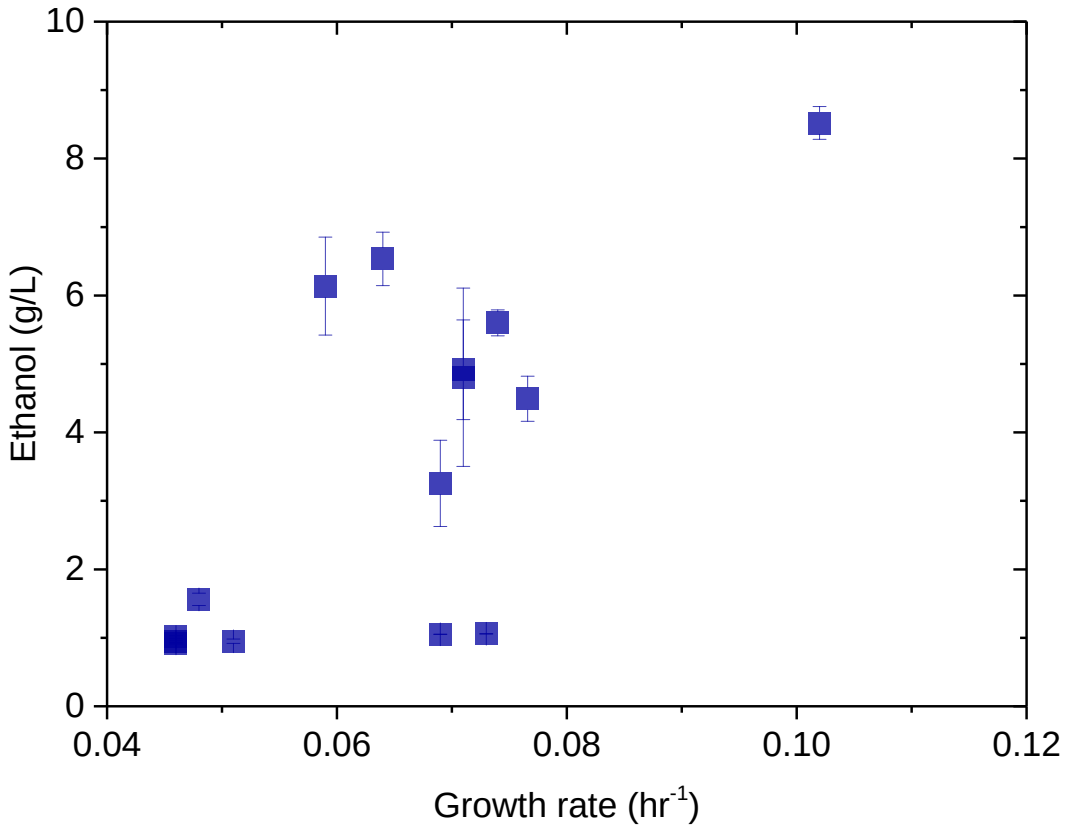

Figure S7. Ethanol concentrations (g/L) at late exponential phase of Y17 strains at different growth rates (1/hr), achieved by varying amounts of dox concentration and induction time, as shown in Table S1. Each data point represents a biological triplicate of an experiment performed at a specific dox concentration, from 0 to 2500 ng/mL, and timing of induction, from OD_{600} 0.01 to OD_{600} 1. Error bars represent standard error among three biological replicates.

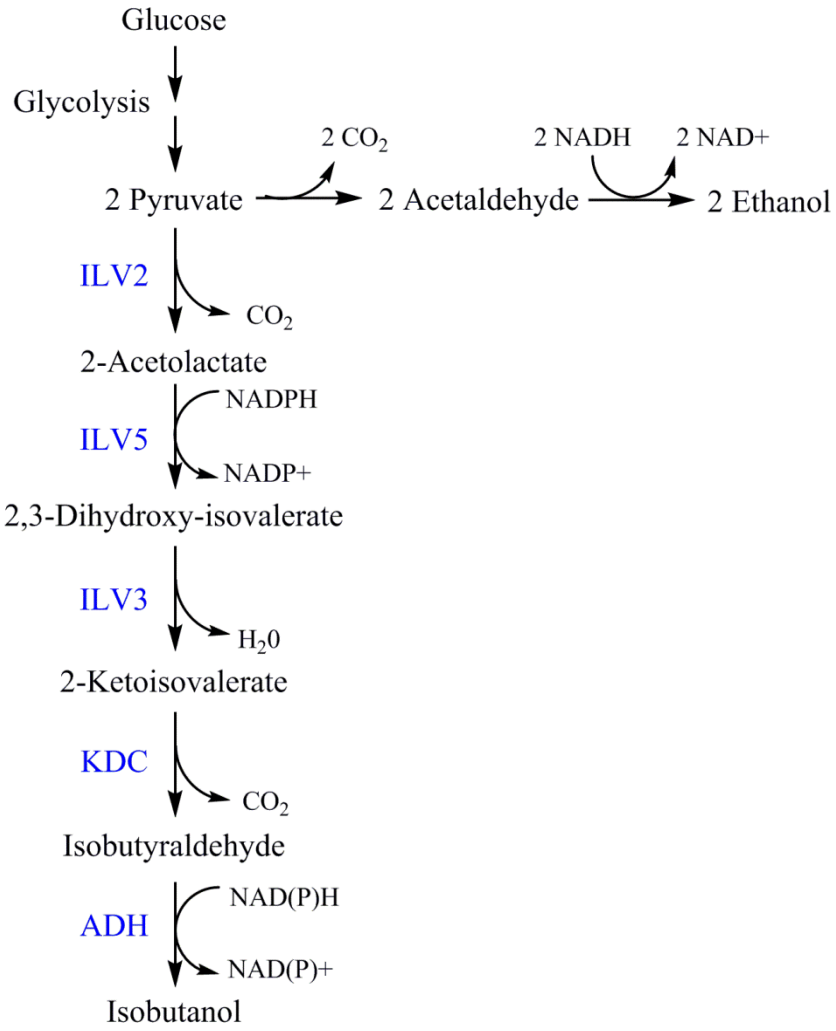

Figure S8. Isobutanol pathway from glucose. Enzyme involved in each conversion step is shown in blue: acetolactate synthase (ILV2), acetohydroxyacid reductoisomerase (ILV5), dihydroxyacid dehydratase (ILV3), keto-acid decarboxylase (KDC), alcohol dehydrogenase (ADH).

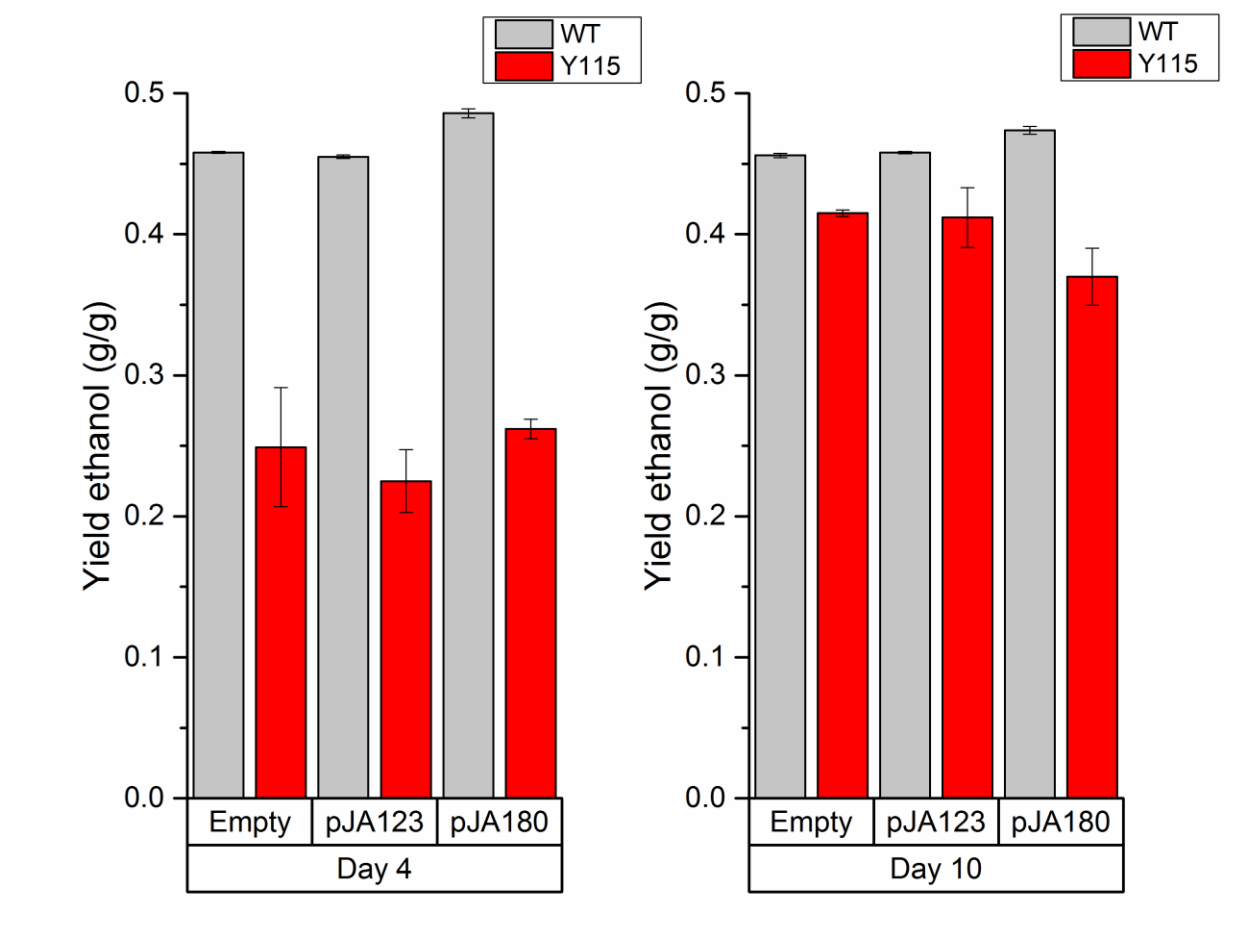

Figure S9. Ethanol yield (g/g glucose) of WT and Y115 cultures with empty pRS426, pJA123 and pJA180, at day 4 and day 10 of culture. Error bars represent standard error among three biological replicates.

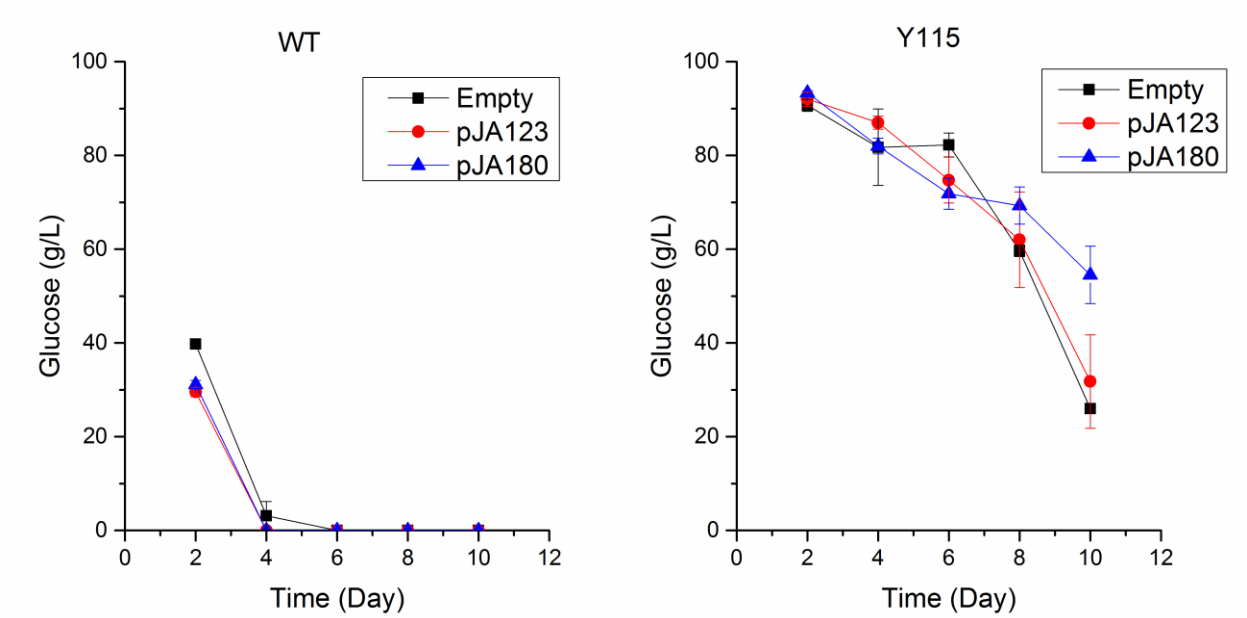

Figure S10. Glucose concentrations (g/L) of WT and Y115 cultures with empty pRS426, pJA123 and pJA180. The initial starting glucose concentration was 100g/L for both WT and Y115. Error bars represent standard error among three biological replicates.

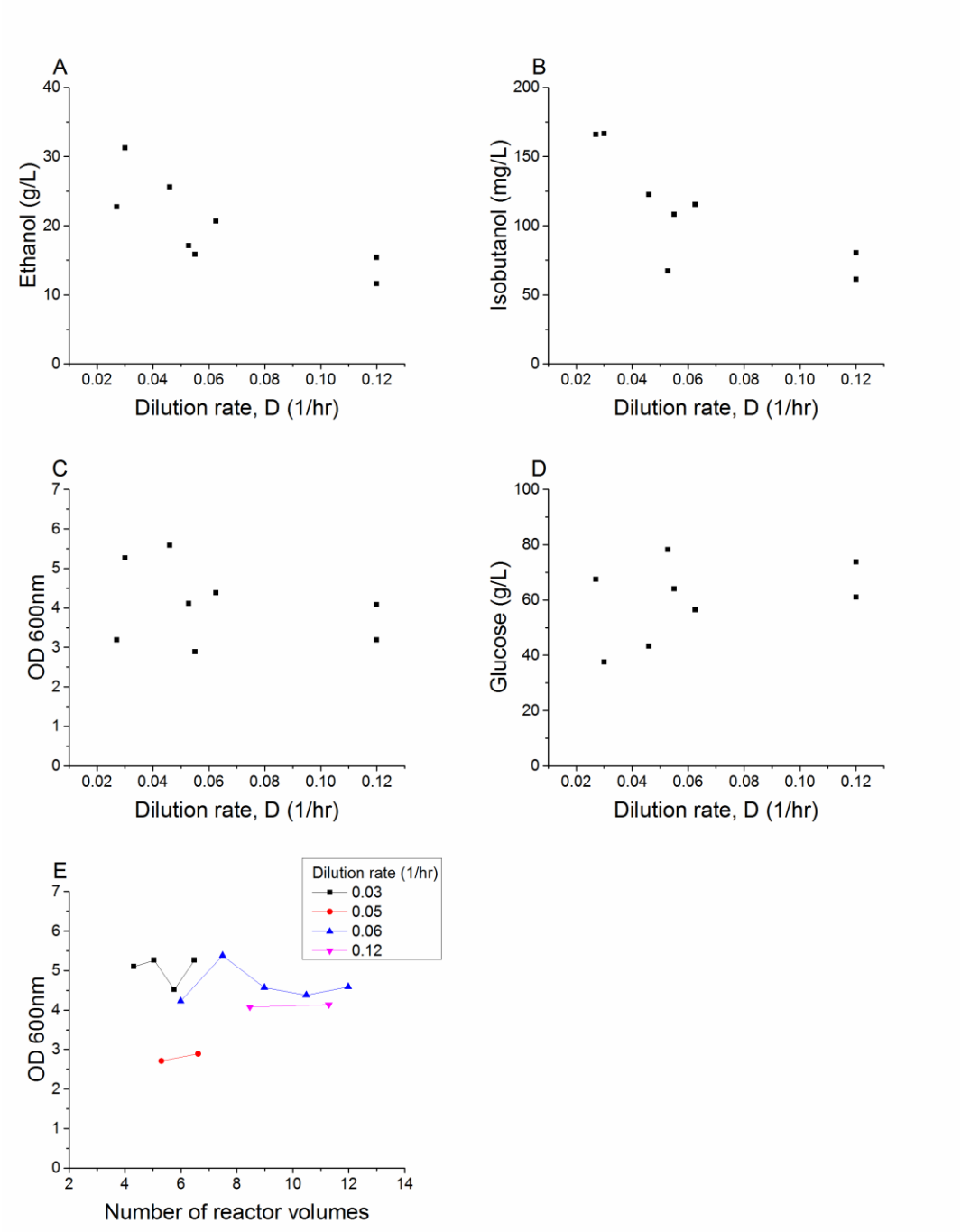

Figure S11. (A) Ethanol (g/L), (B) Isobutanol (mg/L), (C) Optical density (OD_{600}), and (D) Glucose (g/L) concentrations of WT pJA123 at steady state, as a function of dilution rates (1/hr) performed in a continuous stirred tank reactor. (E) Optical density (OD_{600}) of samples taken during the continuous culture of four dilution rates, as a function of the number of reactor volumes that has passed. For example, for D=0.12/hr (25mL reactor flowing at 0.05mL/min), the total volume of flow that has passed at day 3 of is 216 mL, which is 8.6 times the number of reactor volume. Each data point represent a single replicate.

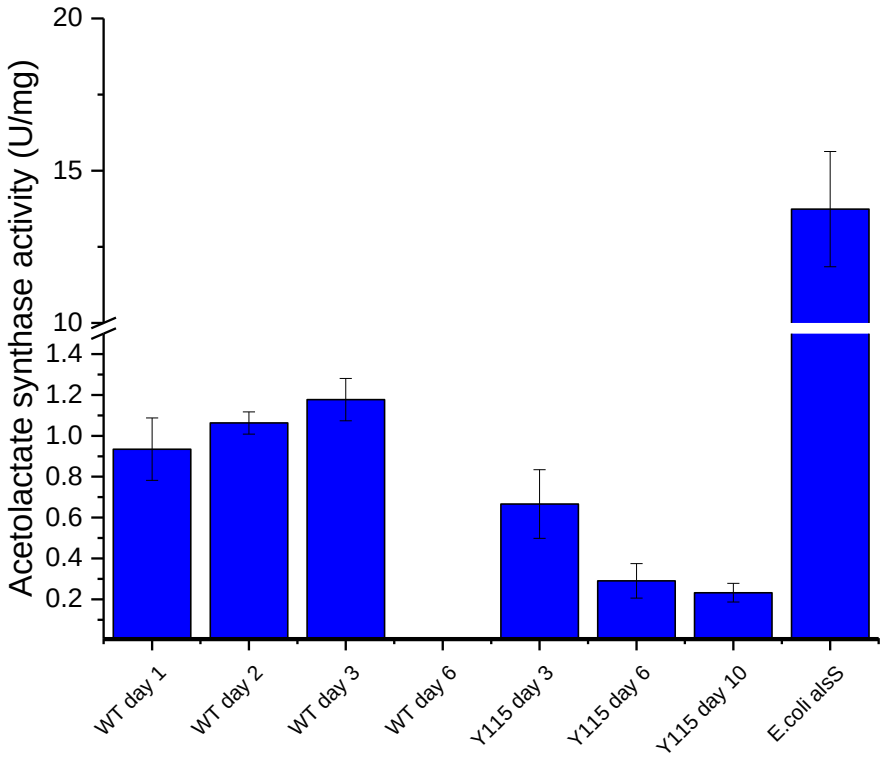

Figure S12. Acetolactate synthase activity (U/mg protein) of WT and Y115 cultures with empty pRS426. *E.coli* overexpressing *alsS* from *B. subtilis* was measured as a positive control. WT samples were taken at days 1, 2, 3 and 6. Y115 samples were taken at days 3, 6, and 10. Error bars represent standard error among three biological replicates.

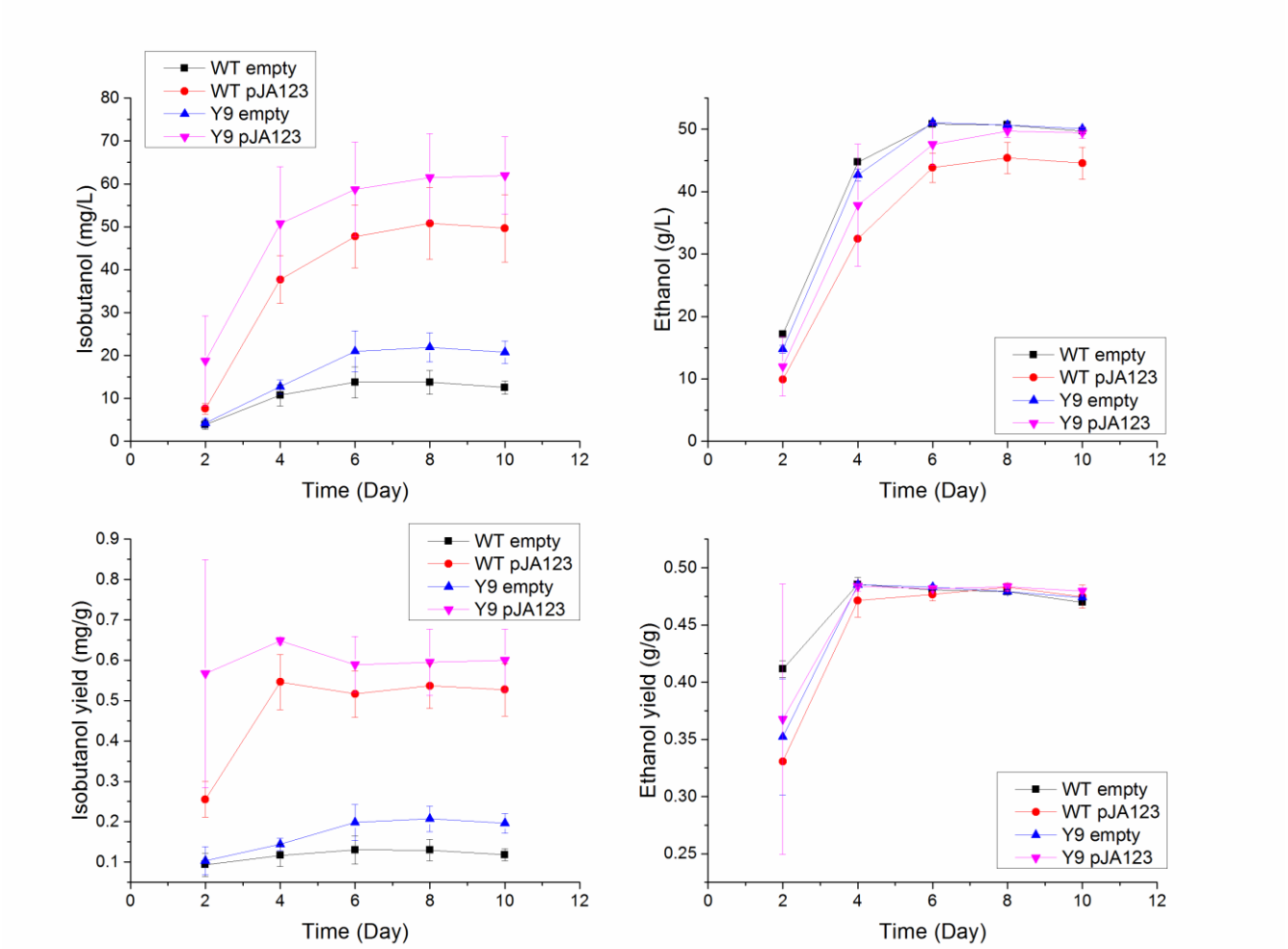

Figure S13. Isobutanol (mg/L), ethanol (g/L), isobutanol yield (mg/g glucose) and ethanol yield (g/g glucose) of WT and Y9 (*hxk2Δ*) strains with empty pRS426 and pJA123. Error bars represent standard error among three biological replicates.

Table S1. Data used for Fig. S5 and S6. Time of induction and dox concentrations used to achieve different growth rates of Y17, with their corresponding gluconate (g/L) and ethanol concentrations (g/L).

Time of induction (OD)	Dox concentrations (ng/mL)	Growth rate (1/hr)	Gluconate (g/L)	Ethanol (g/L)
No induction	0	0.073	0.08	6.14
0.01	250	0.069	0.15	6.53
0.01	500	0.069	1.57	3.26
0.01	1000	0.059	1.63	1.05
0.01	2500	0.064	1.44	1.06
No induction	0	0.071	0.13	4.92
0.1	250	0.071	0.27	4.81
0.1	500	0.046	2.01	0.92
0.1	1000	0.051	1.98	0.95
0.1	2500	0.046	2.07	0.95
No induction	0	0.074	0.05	5.60
0.01	1000	0.046	2.31	1.01
0.15	1000	0.048	1.69	1.56
1	1000	0.077	0.11	4.49
WT strain	0	0.102	0.15	8.52

Table S2. Semi-anaerobic batch cultivations of WT and Y115 strains containing the isobutanol pathway.

Strain	WT CEN.PK2-1D	Y115

Table S2(A). Titers (mM) and OD_{600} of semi-anaerobic batch cultivations of WT and Y115 strains containing the isobutanol pathway.

Strain	WT CEN.PK2-1D			Y115 (CEN.PK2-1D, glk1::KanMX, hxk2::CgHIS3, trp1::7xtetO tTA, HXK1 pr::7xtetO CYC1 TATA)		
	Empty	pJA 123	pJA180	Empty	pJA 123	pJA180
OD_{600}	3.3±0.1	4.06±0.08	3.9±0.3	2.4±0.1	2.52±0.05	1.6±0.1
Isobutanol titers, mM	0.11±0.02	0.71±0.03	0.24±0.03	0.62±0.05	1.7±0.2	2.3±0.1
Ethanol titers, mM	1041±3	1044±2	1046±1	710±13	700±100	410±70
Succinate titers, mM	0.78±0.02	0.85±0.04	0.88±0.03	1.24±0.09	2.9±0.7	1.4±0.4
Glycerol titers, mM	22.5±0.2	22.6±0.5	22.6±0.2	21.2±0.6	20±1	15.2±0.5
Acetate titers, mM	24.7±0.9	23.1±0.5	22.7±0.3	26.1±0.5	22.8±0.4	20±4

				(CEN.PK2-1D, glk1::KanMX, hxk2::CgHIS3, trp1::7xtetO tTA, HXK1 pr::7xtetO CYC1 TATA)		
	Empty	pJA 123	pJA180	Empty	pJA 123	pJA180
Biomass ($CH_{1.78}O_{0.6}N_{0.19}$) yield, mol/mol glucose	0.115±0.005	0.140±0.003	0.134±0.009	0.113±0.004	0.13±0.02	0.12±0.01
Isobutanol yield, mmol/mol glucose	0.19±0.04	1.28±0.05	0.43±0.05	1.5±0.2	4.4±0.2	9.1±0.8
Ethanol yield, mol/mol glucose	1.875±0.006	1.880±0.004	1.885±0.001	1.735±0.008	1.73±0.08	1.61±0.06
Succinate yield, mmol/mol glucose	1.41±0.04	1.54±0.07	1.58±0.05	3.0±0.2	7.3±0.7	5±1
Glycerol yield, mol/mol glucose	0.041±0.001	0.041±0.001	0.041±0.001	0.052±0.001	0.054±0.004	0.062±0.007
Acetate yield, mol/mol glucose	0.044±0.002	0.042±0.001	0.041±0.001	0.063±0.001	0.062±0.007	0.078±0.008

Table S2(B). Molar yields of semi-anaerobic batch cultivations of WT and Y115 strains containing the isobutanol pathway. Biomass, ethanol, glycerol and acetate are in mol/mol glucose. Isobutanol and succinate molar yields are in mmol/mol glucose.

Table S3. Primers used in this study.

Primer	Construct	Sequence
HXK2-CgHIS(-)	HXK2 deletion	GTAGAAAAAGGGCACCTTCTTGTTGTTCAAACTTAAT TTACAAATTAAGTGTTGTAAAACGACGGCCAGT
HXK2-CgHIS(+)		GTTGTAGGAATATAATTCTCCACACATAATAAGTACG CTAATTAAATAAACACAGGAAACAGCTATGACC
GLK1-PrKan(-)	GLK1 deletion	GATGGTAAGTACGGTGGGATACGTACACAAACCAAA AAAATGTAAAAAGAAAACTGGATGGCGGCGGTTAG
GLK1-PrKan(+)		GCTTCCGTAAACCACAACACCACCACTAATACAACTC TATCATACACAAGGATCTGTTTAGCTTGCCTCGTCCC
7xtetO-HXK1(-)	Promoter insertion of 7xtetO TATA at HXK1	GCCATGGAACCCTTTCTAGCCTGTGGTTTCTTTGGAC CTAAATGAACCAT CGAATTGATCCGGTAATTTAG
Pbs-HXK1(+)		TTTTAATCAAACTCACCCAAACAACTCAATTAGAATA CTGAAAAAATAAG TAAAGCACTAAATCGGAACCC
HXK1 A Fwd	Quantification of HXK1 mRNA	GGCTAGAAAGGGTTCCATGGC
HXK1 A Rev		GTTACCTCCCTTCTTTGTCAAACC
GCN4 B Fwd	Quantification of GCN4 mRNA	GTGTTGTTGCTTACAACCGC
GCN4 B Rev		TCGAAAGCAATTCTTCAACC
ILV2 A Fwd	Quantification of ILV2 mRNA	TTCAACATATAGCATACCGC
ILV2 A Rev		GGATCAACATTGAAACTTGG
SNF1 A Fwd	Quantification of SNF1 mRNA	CAATGCAAATTCTAGCCACC
SNF1 A Rev		TAACTTTACCAAAGGACCCC